CHEMISTRY
A EUROPEAN JOURNAL

DOI: 10.1002/chem.201001698

Anionic N-Heterocyclic Carbenes with *N*,*N*′-Bis(fluoroaryl) and *N*,*N*′-Bis(perfluoroaryl) Substituents

Matthew G. Hobbs,[a] Chrissy J. Knapp,[a, b] Patrick T. Welsh,[a] Javier Borau-Garcia,[a] Tom Ziegler,[a] and Roland Roesler*[a]

Dedicated to Professor Hans J. Breunig on the occasion of his 65th birthday

Abstract: A series of rhodium complexes, [Rh(cod)(NHC-F_x)(OH_2)] (cod = 1,5-cyclooctadiene; NHC = N-heterocyclic carbene), incorporating anionic N-heterocyclic carbenes with 2-*tert*-butylmalonyl backbones and 2,6-dimethylphenyl ($x = 0$), 2,6-difluorophenyl ($x = 4$), 2,4,6-trifluorophenyl ($x = 6$), and pentafluorophenyl ($x = 10$) N,N′-substituents, respectively, has been prepared by deprotonation of the corresponding zwitterionic precursors with potassium hexamethyldisilazide, followed by immediate reaction of the resulting potassium salts with [{RhCl(cod)}$_2$]. These complexes could be converted to the related carbonyl derivatives [$Rh(CO)_2$(NHC-F_x)(OH_2)] by displacement of the COD ligand with CO. IR and NMR spectroscopy demonstrated that the degree of fluorination of the *N*-aryl substituents has a considerable influence on the σ-donating and π-accepting properties of the carbene ligands and could be effectively used to tune the electronic properties of the metal center. The carbonyl groups on the carbene ligand backbone provided a particularly sensitive probe for the assessment of the metal-to-ligand π donation. The *ortho*-fluorine substituents on the *N*-aryl groups in the carbene ligands interacted with the other ligands on rhodium, determining the conformation of the complexes and creating a pocket suitable for the coordination of water to the metal center. Computational studies were used to explain the influence of the fluorinated N-substituents on the electronic properties of the ligand and evaluate the relative contribution of the σ- and π-interactions to the ligand–metal interaction.

Keywords: carbenes · donor–acceptor systems · ligands · NMR spectroscopy · rhodium

Introduction

As a result of their excellent two-electron donor ability, synthetic accessibility, stability, and tunability,[1] N-heterocyclic carbenes (NHCs)[2] have grown into a highly successful and versatile class of ligands[3] with extensive applications in coordination chemistry and catalysis.[4] Substantial efforts have been invested towards improving their electron-donor ability and, therefore, several methods for the assessment of this property have been devised.[5] Extensive computational[6] and detailed experimental[7] studies have shown that π interactions can also play a significant role in the bonding of these classical σ donors to transition metals[8] and influence the proficiency of metal-based catalytic systems incorporating such ligands.[6c] Motivated by the desire to better tune the electronic properties of the metal centers in complexes incorporating NHCs as ancillary ligands, and to better understand the bonding of these ligands to metals, we set out to prepare highly fluorinated NHCs bearing *N*-polyfluorophenyl groups. These substituents are expected to lower the energy of the LUMO, and hence improve the π-accepting ability of the ligands, strengthening the M–C bond, and reducing the electron density on the metal in their complexes. Fluorinated substituents have been used to this end with phosphines.[9]

[a] M. G. Hobbs, C. J. Knapp, P. T. Welsh, J. Borau-Garcia, Dr. T. Ziegler, Dr. R. Roesler
Department of Chemistry, University of Calgary
2500 University Dr. NW, Calgary, Alberta, T2N 1N4 (Canada)
Fax: (+1) 403-289-9488
E-mail: roesler@ucalgary.ca

[b] C. J. Knapp
Current address: Department of Chemistry
University of Alberta, 11227 Saskatchewan Dr.
Edmonton, Alberta, T6G 2G2 (Canada)

Supporting information for this article is available on the WWW under http://dx.doi.org/10.1002/chem201001698.

Several complexes of carbenes incorporating N-fluorinated substituents have been reported, including symmetrically substituted derivatives bearing 4-fluorophenyl substituents, **A**[10] and **C**,[11] and unsymmetrically substituted ligands bearing 2,6-difluorophenyl groups, **D**.[12] Ruthenium complexes featuring the symmetrically substituted **E**[13] and **B**,[14] the unsymmetrically N-substituted **F**,[15] as well as the most highly fluorinated analogue reported to date, **G**,[16] containing a pentafluorophenyl and a mesityl N-substituent, have been shown to be competent catalysts in olefin metathesis reactions. The $[RhCl(CO)_2(NHC)]$ complexes incorporating the less highly fluorinated NHC **E** exhibit higher frequency ν_{CO} stretching vibrations than the corresponding analogues containing **G**, which indicates that the former ligand is a poorer electron donor than the latter, despite of its lower fluorine content. The electronic influence of the pentafluorophenyl substituent in **G** is likely tempered by that of its more electron-rich *N*-mesityl substituent. NHCs bearing *N*-fluoroalkyl and fluorobenzyl groups have also been reported;[17] however, the hydrocarbon bridges required to tether the fluorinated substituents to the heterocyclic moieties in these compounds diminish their electronic influence on the carbene center.

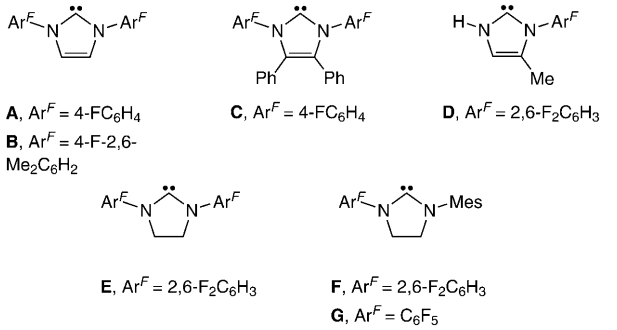

The low number of reported NHCs with fluorinated N-substituents is likely due in part to the strongly σ-donor nature of carbene ligands in general, which enticed efforts to further enhance this property through the use of electron-donating substituents. The use of electron-withdrawing substituents is also expected to lead to a decreased HOMO–LUMO gap in the free ligands, and hence a decrease in their stability. Aside from this however, the classical [4+1] ring-closing reactions commonly employed for the synthesis of NHC precursors, such as imidazolium salts, are ineffective for the synthesis of analogues featuring highly fluorinated N-substituents, owing to the poor nucleophilicity of the highly fluorinated ethylenediamine or diazabutadiene starting materials. We have shown that the [3+2] ring-closing reactions of easily accessible nonfluorinated as well as poorly nucleophilic, fluorinated, and perfluorinated *N,N*-bis(phenyl)formamidines[18] with highly electrophilic oxalyl chloride proceeds readily to give molecular products **H** instead of the expected ionic derivatives **I**.[19] These molecular products **H** displayed reactivity typical of alkyl halides, and in our hands failed to generate the targeted NHCs, **J**. Computational analyses showed that the oxalamide backbone significantly lowered the energy of the LUMO of the desired carbenes **J**, increasing their π-acceptor (electrophilic) character and decreasing their stability to the point where it rendered them too instable for isolation. Meanwhile, a series of closely related amido and diamidocarbenes have been isolated or incorporated in transition-metal complexes, including the anionic carbenes **K**,[20] the neutral derivatives **L**,[21] and the five-membered monoamidocarbenes **M**.[22]

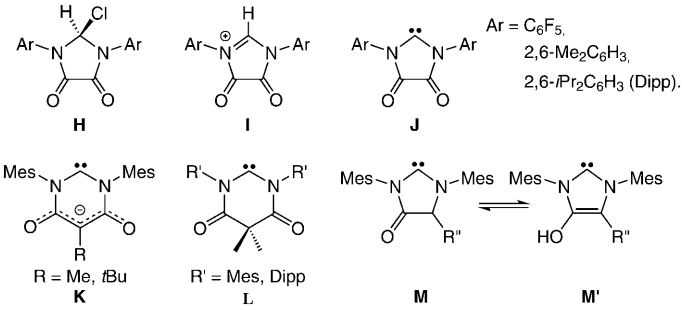

Although carbenes **K**–**M** are highly reactive compounds, it is clear that the destabilizing influence of the amido functionalities on the amidocarbene moiety in these compounds is inferior in magnitude to that observed in the oxalamide ligands **J**. The anionic framework of **K**, formally obtained by the insertion of a CR^- fragment between the backbone carbon atoms of unstable analogues **J** in particular appears to be a viable scaffold for the synthesis of the symmetric NHCs featuring *N,N′*-bis(fluoroaryl) substituents, NHC-F_4^-, NHC-F_6^-, and NHC-F_{10}^-. The delocalization of the anionic charge over the carbonyl-containing backbone of **K** is expected to enhance the stability of the carbene center, while retaining the synthetic advantage presented by the high electrophilicity of malonyl chloride, which allows for ring-closing reactions using poorly nucleophilic fluorinated *N,N′*-bis(phenyl)formamidines. Additionally, the carbonyl func-

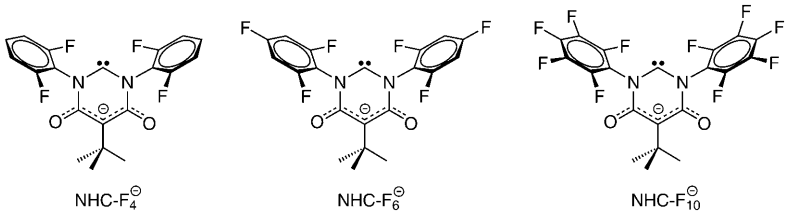

tions adorning the backbone of **K** provide a sensitive probe for the evaluation of the effect of metal back-donation onto the π framework of the ligand. The use of carbonyl and cyano functionalities on the ligand backbone for the assessment of π-accepting properties of NHCs has been reported.[7] In addition to the fluorinated carbenes depicted, the nonfluorinated analogue NHC-F_0⁻ bearing *N,N′*-bis(2,6-dimethylphenyl) substituents was targeted as well, to serve as a reference.

Results and Discussion

The condensation reaction of 2-*tert*-butylmalonyl dichloride with *N,N′*-bis(aryl)formamidines proceeded smoothly at room temperature in THF in the presence of triethylamine, yielding the zwitterionic precursors **1a–d**, which were isolated as yellow solids (Scheme 1). The NMR spectra of these

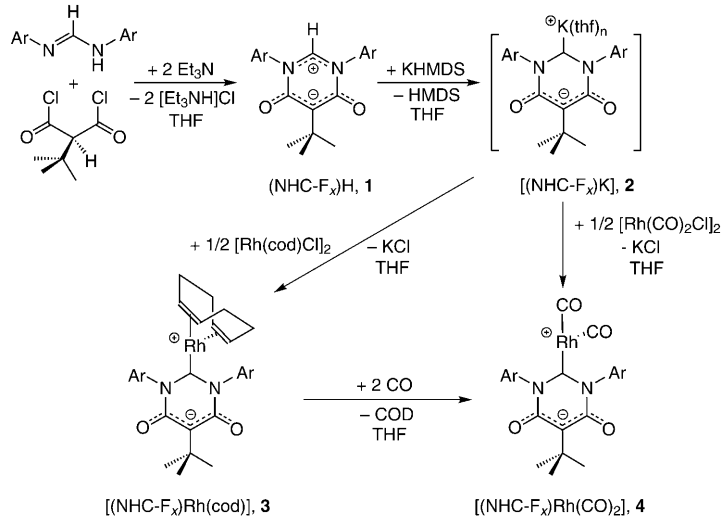

Ar = 2,6-$Me_2C_6H_3$, *x* = 0, **a**; 2,6-$F_2C_6H_3$, *x* = 4, **b**; 2,4,6-$F_3C_6H_2$, *x* = 6, **c**; C_6F_5, *x* = 10, **d**.

Scheme 1. Synthesis of rhodium complexes **3** and **4** and of their precursors **1** and **2**.

derivatives featured all the signals expected for a C_{2v} symmetry, and the symmetric stretching vibrations corresponding to the carbonyl groups were clearly distinguishable at 1668.6, 1679.6, 1683.4, and 1681.3 cm^{-1} for **1a–d**, respectively.

A crystallographic determination for **1c** revealed the expected planar framework (Figure 1) and confirmed the zwitterionic structure outlined in Scheme 1. The C(1)–N(1) and C(1)–N(2) bonds measure 1.311(3) and 1.315(3) Å (Table 1, cf. 1.34 Å in pyridine),[23] identical to the

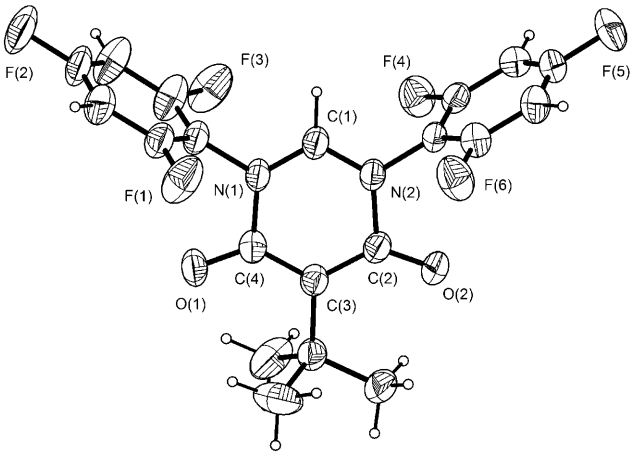

Figure 1. Molecular structure of **1c** with 50% probability level thermal ellipsoids.

corresponding bonds observed in imidazolium and dihydroimidazolium ions (1.324(14) Å),[24] as well as the zwitterionic precursor to **K** (R = Me, 1.314(3) and 1.317(3) Å).[20] The C(3)–C(2) and C(3)–C(4) bonds of the backbone are also short, with distances of 1.410(3) and 1.418(3) Å (cf. 1.40 Å in benzene),[25] in agreement with the extensive electron delocalization over the N–C–N and C–C–C fragments of the framework. The N(1)–C(4) and N(2)–C(2) bonds (1.476(3) and 1.487(3) Å, respectively) are very long for amide functionalities, and much longer than the corresponding distances observed in the molecular derivatives **H** (1.348(5)–1.381(2) Å)[19] or in hexamethylmalonamide (1.34 Å).[26] As observed in the precursor to **K**,[20] the competitive delocalization over the C–C–C backbone in **1a–d** reduces the multiple-bond character of the amidic C–N bond. This allows for a better delocalization of the nitrogen lone pairs over the N–C–N moiety than in analogue **H**, and the consequent stabilization of the amidinium structure over a neutral molecular structure. A precursor to **L**, which lacked any such competitive delocalization, was observed to feature a neutral molecular structure similar to that observed for **H**,[21b] supporting this assertion.

In the presence of potassium hexamethyldisilazide (KHMDS) the precursors **1b–d** were easily deprotonated in THF, yielding the highly reactive potassium salts **2b–d** of the targeted anionic NHCs. Derivatives **2c** and **2d** decom-

Table 1. Selected bond lengths [Å] and angles [°] for **1c**, **3b**·H_2O, **3c**·H_2O, and **3d**·H_2O.

	1c	**3b·H_2O**	**3c·H_2O**	**3d·H_2O**
Rh(1)–C(1)	–	2.043(4)	2.040(6)	2.047(5), 2.051(6)
Rh(1)–O(3)	–	2.138(4)	2.149(5)	2.147(4), 2.152(5)
O(3)···F	–	2.888(6), 2.960(5)	2.802(6), 2.941(7)	2.993(7)–3.059(6)
C(24,25)···F	–	3.369(6), 3.374(6)	3.354(8), 3.374(9)	3.168(8)–3.833(10)
C(1)–N	1.311(3), 1.315(3)	1.351(5), 1.360(6)	1.347(7), 1.358(7)	1.336(6)–1.357(6)
N–C(O)	1.476(3), 1.487(3)	1.451(6), 1.458(6)	1.452(7), 1.466(7)	1.462(6)–1.482(6)
C(3)–C(O)	1.410(3), 1.418(3)	1.412(6), 1.416(6)	1.403(8), 1.415(8)	1.393(7)–1.411(7)
C–O	1.220(3), 1.224(3)	1.234(5), 1.240(6)	1.240(7), 1.242(7)	1.229(6)–1.234(7)
N(1)-C(1)-N(2)	120.2(2)	112.9(4)	113.3(5)	112.4(4), 112.7(4)

posed quickly in solution to unidentified products, eluding isolation and characterization, but could be converted immediately to the rhodium complexes **3c**,**d** and **4c**,**d**. The formation of the more stable **2b**, which could be isolated as a yellow solid, was followed by NMR spectroscopy and revealed the existence of two forms in solution in a ratio of approximately 2:1: a more abundant C_{2v}-symmetric species and a less symmetric species with C_2 or C_s symmetry. The crystal structure reported for the analogous lithium salt of ligand $\mathbf{K}_{Me}$ showed a trimeric associate [{Li($\mathbf{K}_{Me}$)(thf)$_2$}$_3$] featuring Li–O but no Li–C contacts,[20] and hence it is likely that in THF solution **2b** exists in two forms differing in the degree of association, or in the coordination mode to the potassium ions, via the carbene carbon or the amide oxygen atoms. The reaction of this salt with rhodium chloride complexes resulted in practically quantitative formation of **3b** or **4b**, respectively, proving that the two species observed in solution are two forms of the same compound (Scheme 1). The signal corresponding to the carbene carbon atom in the ^{13}C NMR spectrum of **2b** appeared at $\delta = 244.5$ ppm for the major constituent, considerably downfield shifted with respect to the resonance of the N_2CH carbon atom in the zwitterionic precursor **1b** ($\delta = 156.6$ ppm). The corresponding resonance for the minor constituent could not be located.

Complexes **3a–d** were produced cleanly in the reaction of in situ generated **2a–d** with a stoichiometric amount of [{RhCl(cod)}$_2$] in THF (cod = 1,5-cyclooctadiene). The new complexes were only soluble in strongly polar donor solvents, such as THF and especially DMSO. Their solubility increased with the degree of fluorination; from **3a** (Ar = 2,6-$Me_2C_6H_3$), which upon formation immediately deposited out of the THF solution in form of orange crystals, to **3d** (Ar = C_6F_5), which was well-soluble in the same solvent. All complexes were prepared under anhydrous conditions but the derivatives containing fluorinated substituents showed a high affinity for water and readily formed the adducts **3b–d**·H_2O during isolation and characterization. It could not be conclusively determined if the water remained coordinated in solution and the mass spectra for all compounds featured molecular ions for **3b–d** alone. The NMR spectra of these complexes, independent from the presence or absence of water, were in agreement with the C_s-symmetric structures **3II** and **3**·H_2O, respectively. A structure such as **3I**, which was observed in the solid state but not in solution for [Rh(cod)($\mathbf{K}_{Me}$)],[20] could not be completely ruled out. In fact, a computational study for a model compound showed, for example, structure **3I** to be 2.8 kcal mol^{-1} more stable than **3II** (see the Supporting Information). However, given that compounds **3b–d** only dissolve in coordinating solvents (THF, DMSO), the most probable solution structure features a donor molecule, such as water or solvent occupying the free coordination site of the square-planar rhodium center, as shown for **3b**·H_2O. Through-space coupling was observed in the ^{13}C NMR spectra of **3b–d** between one of the two sets of nonequivalent *ortho* fluorine nuclei on the aryl groups and the cyclooctadiene carbon atoms bonded *cis* to the carbene ligand ($J_{CF} = 9$ Hz). This supports the assignment of

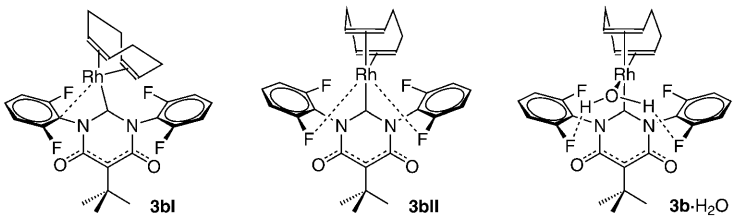

structure **3**·(donor) and indicates that no fast dynamic processes involving rotation around the Rh–C_{NHC} bond takes place at this temperature. Through-space carbon–fluorine coupling of a similar magnitude has been reported[27] and the alternative of a through-bond coupling involving the other of the two sets of nonequivalent *ortho* fluorine nuclei in structure **3II** was rejected based of the lack of an observable $^1J_{RhF}$ coupling. The resonance corresponding to the carbene carbon atom in **3a–d** appeared as a doublet with a $^1J_{RhC}$ coupling constant of 47.9–49.4 Hz at $\delta = 206.2$, 211.8, 212.7, and 215.2 ppm, respectively.

Derivatives **3b–d** showed a high propensity to crystallize only in the presence of adventitious water as **3b–d**·H_2O and could be characterized by means of single-crystal X-ray diffraction. The determinations revealed very similar structures for all three complexes (Figures 2–4), featuring pseudo-

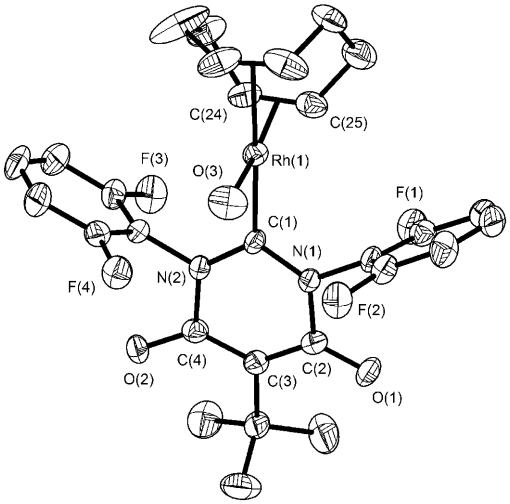

Figure 2. Molecular structure of **3b**·H_2O with 50% probability level thermal ellipsoids. All hydrogen atoms have been omitted for clarity.

square-planar rhodium centers coordinated by the carbene ligand, a water molecule, and cyclooctadiene, with the plane of the metal nearly perpendicular to the ligand framework as shown for **3b**·H_2O. The observed geometry formally allows for efficient π-back-bonding from a filled metal orbital (d_{xy}) to the vacant p orbital present on the carbenic center. This is in strong contrast to the analogous complex [Rh(cod)($\mathbf{K}_{Me}$)] reported by César and Lavigne, which in the solid state displayed a structure very similar to **3bI**.[20] The plane of the strongly distorted pseudo-square-planar

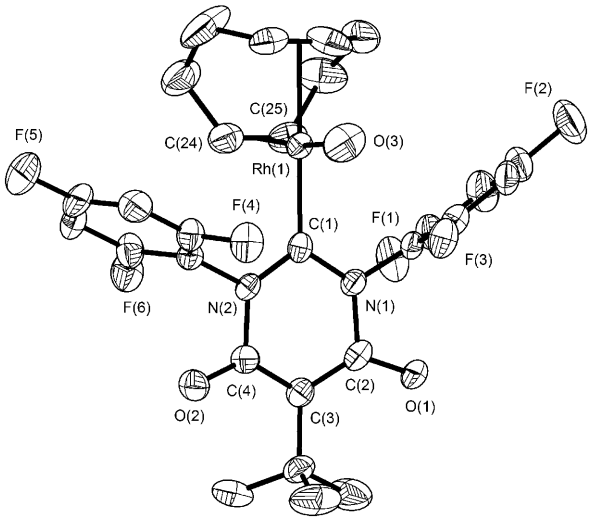

Figure 3. Molecular structure of **3c**·H_2O with 50% probability level thermal ellipsoids. All hydrogen atoms have been omitted for clarity.

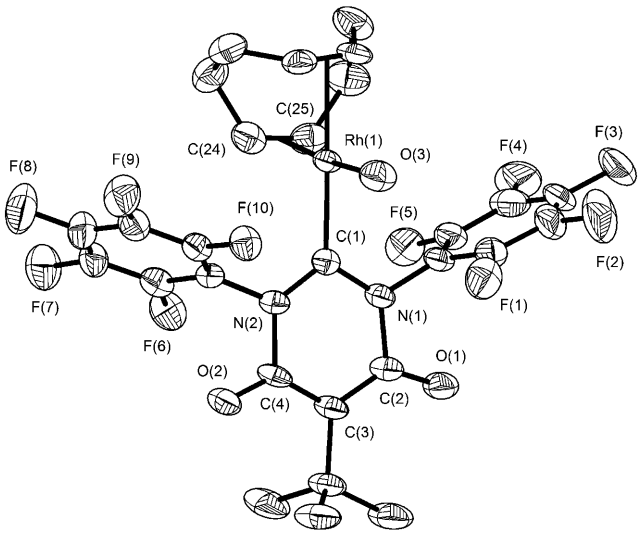

Figure 4. Structure of one of the two independent molecules of **3d**·H_2O in the crystal with 50% probability level thermal ellipsoids. All hydrogen atoms have been omitted for clarity.

metal in this water-free complex nearly coincided with the main plane of the ligand and the metal was strongly drawn towards one of the mesityl groups by a π interaction (Rh–C_{ipso} = 2.346 vs. Rh···C_{ipso} = 3.706 Å for the two mesityl groups, respectively). The C(1)–Rh(1) distances in **3b–d** measured between 2.040(6) and 2.051(6) Å, comparable to the average distances observed in NHC complexes of rhodium (2.028(2) Å).[24]

Minor changes in the structure of the ligand skeleton were observed upon coordination, including a slight lengthening of the intraannular C(1)–N bonds (1.311(3), 1.315(3) in **1c** vs. 1.347(7), 1.358(7) Å in **3c**·H_2O, respectively) and a narrowing of the N-C-N angle involving the carbene carbon atom (120.2(2) in **1c** vs. 113.3(5)° in **3c**·H_2O, respectively). These changes mirror those generally observed upon coordination of NHC ligands. In all compounds, two of the *ortho* fluorine atoms were situated close to the cyclooctadiene carbon atoms bonded *cis* to the carbene ligand (F···C 3.168(8)–3.833(10) Å, see Table 1), as proposed based on the through-space carbon–fluorine coupling observed in the ^{13}C NMR spectra. These types of interactions have been investigated extensively and it was concluded that they are very weak hydrogen bonds (ca. 0.43 kcal mol^{-1}).[28] The other two *ortho* fluorine atoms were situated in the proximity of the water molecule (F···O 2.802(6)–3.059(6) Å). Although the hydrogen atoms in water could not be located, these distances and the geometric arrangement (F···O···F 94.0(2)–111.0(2)°) indicate the likely presence of F···H–O hydrogen bonding. Numerous reports describe the presence of such weak interactions in similar structural arrangements and emphasize their importance in crystal engineering, although the frequency of their occurrence has been the object of some debate.[29] The systematic presence of coordinated water in the solid-state structures of **3b–d**·H_2O is interesting, given that the very similar [Rh(cod)(**K**$_{Me}$)] adopted a water-free solid-state structure similar to **3bI**, although its preparation involved an aqueous workup.[20] Several factors are likely to contribute to this notable difference in reactivity. The fluorinated groups diminish the electron donor ability of the ligand, reducing the electron density of the 14-electron rhodium center and increasing its Lewis acidity. The perfluorinated groups are also less electron rich than the mesityl substituents in **K**$_{Me}$, and are able to provide less electron density in a π interaction such as the one observed in [Rh(cod)(**K**$_{Me}$)]. No less important, the F···H–O hydrogen bonding proposed in **3b–d**·H_2O contributes to the stabilization of the water-containing product in a suitable coordination pocket. Computational treatment of a model compound shows that the rotation of the water ligand by 180° around the Rh–O bond, which involves the cleavage of both F···H–O hydrogen bonds, results in an increase in energy of approximately 8.1 kcal mol^{-1} (see the Supporting Information). This demonstrates that the stabilizing influence of this secondary bonding is sizeable.

The steric demand of NHCs has a considerable influence on their stability, ligand properties, and proficiency as ancillary ligands in catalytic systems, and consequently it has been extensively investigated.[3d,4l,5g,30] The use of fluorinated, electron-withdrawing N-substituents in the NHCs targeted in this manuscript was expected to result in decreases in the energy of the LUMO, as well as the HOMO–LUMO gap of these ligands, and consequently to a decrease in stability. For this reason, the assessment of the steric protection provided by the fluoroaryl groups was of particular interest. The recently introduced concept of percent buried volume (% V_{bur}) provided a convenient tool to this end.[31] The data obtained for compounds for which the carbene is coordinated to fragments with small steric demand (such as the proton) suggests that diamidocarbenes with backbones derived from malonic acid (NHC-F_n^- (n = 0, 4, 6, and 10), **K** and **L**) are sterically demanding. As a result, % V_{bur} values

determined for these ligands were 6–8% higher than those measured for imidazolidin-2-ylidenes, such as IMes (*N,N'*-dimesityl substituted) and IPr (*N,N'*-bis(2,6-diisopropylphenyl) substituted), with identical substitution patterns at nitrogen (Table 2). This is expected given the influence of the ligand

Table 2. Percent buried volume values (% V_{bur}) calculated for ligands NHC-F_n^- ($n=4$, 6, 10), as well as for related ligands **K** and **L** and several reference compounds.[31]

NHC	% V_{bur} for M–C at 2.00/2.28 Å (NHC)X	[Rh(cod)(L)(NHC)]	[M(L)$_n$(NHC)]
NHC-F_4^-	–	37.8/32.9[a]	–
NHC-F_6^-	42.2/37.3[b]	39.1/34.3[a]	–
NHC-F_{10}^-	–	37.1/32.4[a]	–
$\mathbf{K}_{Me}$[20]	44.0, 46.3/38.7, 41.1[b]	–	43.2/37.9[c]
$\mathbf{K}_{tBu}$[20]	44.5/39.2[d]	–	36.4/31.2[e]
$\mathbf{L}_{Dipp}$[21a]	53.9/48.6[f]	–	39.3/34.1[g]
$\mathbf{L}_{Mes}$[21b]	–	38.4/33.2[h]	40.3/34.9[i]
IPr	47.3/41.8[f][32]	34.1/29.0[h][34]	–
IMes	36.7/31.5[f][33]	33.5/28.5[h][35]	–

[a] L = H_2O. [b] X = H. [c] ML_n = Rh(cod). [d] X = Ag(PPh_3). [e] [Fe(CO)$_2$Cp(NHC)]. [f] X = H^+. [g] [IrCl(cod)(NHC)]. [h] L = Cl. [i] ML_n = S.

skeleton (a six-membered ring in the ligands discussed herein vs. a five-membered ring in imidazolidin-2-ylidenes) on the dihedral angle between the *N*-aryl substituents. According to this evaluation method, the steric demand of the ligands incorporating fluoroaryl groups is only slightly inferior to that of their analogues featuring methylated phenyl groups of comparable symmetry (e.g. 2,4,6-trifluorophenyl in NHC-F_6^- vs. mesityl in **K**). Finally, it appears that the diamidocarbene ligands are slightly more rigid than the imidazolidin-2-ylidenes, deforming less under the pressure of sterically demanding metal fragments, such as {M(cod)(L)} (M = Rh, Ir; L = Cl^-, H_2O).

Complexes **4a–d** could be prepared either from **3a–d** by displacement of the 1,5-cyclooctadiene ligand by using carbon monoxide, or by salt metathesis reaction of the in situ generated **2a–d** with [{RhCl(CO)$_2$}$_2$] (Scheme 1). The products could be isolated as yellow solids but their stability in solution was not sufficient to allow for the growth of single crystals suitable for X-ray diffraction. Depending on the synthetic method, as well as the water content of the starting materials (**1a–d** or **3a–d**·H_2O) and solvents, **4a–d** could be prepared anhydrous or hydrated. In the absence of conclusive crystallographic, mass spectrometric, or NMR spectroscopic evidence, however, it could not be established experimentally if the water was coordinated to rhodium, as observed in the solid-state structures of **3b–d**·H_2O. Aside from the expected changes resulting from the modifications in the substitution pattern of the rhodium center, the NMR signature of complexes **4a–d** was very similar to that of **3a–d**, which suggests similar structures. Accordingly, structures, such as **4b**·D (D = THF, DMSO) and **4b**·H_2O were proposed for the anhydrous and hydrated forms of these compounds. The ^{13}C NMR spectroscopic resonance corresponding to the carbene carbon atom in **4a–d** appeared as a doublet with a $^1J_{RhC}$ coupling constant of 40–42 Hz in a narrow range between $\delta = 199$ and 203 ppm. As with complexes **3b–d**, through-space coupling between one of the two sets of nonequivalent *ortho* fluorine nuclei on the aryl groups and the carbon nuclei in the carbonyl groups bonded *cis* to the carbene ligand was observed in the ^{13}C NMR spectra of **4b–d**, resulting in a doublet ($^1J_{RhC}$ = 73–76 Hz) of triplets (J_{CF} = 4 Hz) splitting and supporting the geometry of the proposed structures.

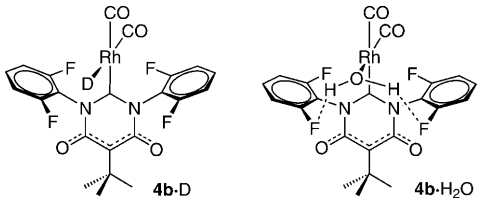

The IR stretching vibrations corresponding to the carbonyl groups in [RhCl(CO)$_2$(L)] and [IrCl(CO)$_2$(L)] complexes have been used extensively for the assessment of the donor ability of phosphine and NHC ligands L.[5] Table 3 presents

Table 3. Compilation of ν(CO) values for selected Ir and Rh–NHC complexes [cm^{-1}][a]

Complex	ν(CO)	ν_{av}(CO)Rh[b]	Ref.
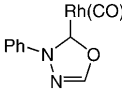	2020, 2098[c]	2059	[36]
4d·H_2O	2015.4, 2091.2[c]	2053.3	
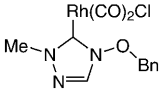	2012, 2090[c]	2051	[36]
4c·H_2O	2015.2, 2085.0[c]	2050.1	
[$IrCl(CO)_2(M_{Ph})$]	1989.5, 2075.8[d]	2049.3[e]	[22b]
[$IrCl(CO)_2(L_{Dipp})$]	1991, 2074[d]	2049.1[e]	[21a]
[$IrCl(CO)_2(M_{tBu})$]	1989.0, 2075.1[d]	2048.6[e]	[22b]
4b·H_2O	2013.1, 2083.3[c]	2048.2	
[$RhCl(CO)_2(L_{Mes})$]	2005.3, 2086.1[d]	2045.4	[21b]
[$RhCl(CO)_2$(IMes)]	2006, 2076[d]	2041	[37]
[$RhCl(CO)_2$(SIMes)]	1996, 2081[d]	2039	[37]
4a·H_2O	1994.9, 2074.4[c]	2034.7	
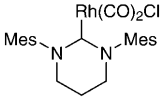	1976, 2062[c]	2019	[38]

[a] The direct comparison between the numeric values for [RhCl(CO)$_2$(NHC)] and [Rh(CO)$_2$(H_2O)(NHC)] complexes is to be treated with caution. [b] For Ir complexes the conversion $\nu_{av}(CO)Rh = 1.150 \cdot \nu_{av}(CO)Ir - 288.3$ cm^{-1} was used.[5f] [c] KBr pellets. [d] CH_2Cl_2 solution. [e] Calculated.

the pertinent data for complexes **4a–d**·H_2O, together with a selection of reference compounds. It is evident that the degree of fluorination of the NHC-F_x^- ligands has a direct and notable influence on the electron density of the rhodium center. The expected trend is observed for the average frequency ν_{av}(CO)Rh, which increases from 2034.7 for

4a·H_2O to 2053.3 cm^{-1} in **4d**·H_2O, which indicates a decrease in electron density on the metal. A difference of approximately 20 wavenumbers is considerable on this narrow scale, matching for example the difference exhibited by complexes incorporating five- and six-membered NHCs with saturated backbones (Table 3). This clearly demonstrates that the fluorination of the *N*-aryl substituents is an efficient tool for tuning the electronic properties of NHCs. The degree of fluorination has a smaller, albeit consistent impact on the rhodium center coordinated to the NHC, with the complexes incorporating ligands NHC-F_0^- and NHC-F_4^- separated by 13.5 cm^{-1} on this scale, whereas those containing ligands NHC-F_4^- and NHC-F_{10}^- are only 5.1 cm^{-1} apart. An immediate comparison between the electronic properties of anionic NHCs, such as NHC-F_x^-, and those of neutral carbenes by using the values of the IR vibrations observed in metal complexes is precluded by the different structures of these complexes, that is, $[RhCl(CO)_2(NHC)]$ versus $[Rh(CO)_2(H_2O)(NHC)]$. It has been shown for example that even the nature of the halogen in $[Rh(CO)_2(NHC)X]$, X = Cl, I has an influence, albeit very small, on the respective ν_{av}(CO)Rh values.[5c] For the same reason, no attempts have been made to calculate Tolman's electronic parameter, which can be derived from data obtained for $[MCl(CO)_2(NHC)]$ (M = Rh, Ir) complexes.[5e] More important than the comparison between the ligands properties is the comparison between the electronic properties of the metal centers in their complexes. The data featured in Table 3 clearly demonstrates that the electron density on the rhodium center in **4b–d**·H_2O is lower than in most $[RhCl(CO)_2(NHC)]$ complexes. It can be concluded that, like other amidocarbenes, such as **L** and **M**, the new ligands NHC-F_x^- described herein are comparatively weak electron donors.

As mentioned in the introduction, the assessment of the π-accepting ability of NHC ligands, as well as of the tunability of this property by means of fluorination was also of interest. The symmetric stretching vibration of the carbonyl functionalities on the ligand backbone is expected to be sensitive to electron donation into the π-system of the ligand, and shows little dependence on the electron effects within the σ-framework. This has been previously demonstrated for NHC ligands featuring carbonyl and cyano groups attached to the ligand framework.[7] As expected, the zwitterionic precursors **1a–d** containing the carbene ligand formally coordinated to a proton (and hence not experiencing any π-back-donation) display the highest values for the $\nu(CO_{backbone})$ vibration (Table 4). The lowest vibration frequencies corresponding to the CO backbone are observed for complexes **3a–d**·H_2O, in which the poor π-accepting ability of the 1,5-cyclooctadiene and water ligands renders the rhodium center more electron rich, resulting in stronger π-back-donation from the metal to the carbene ligand. Generally, for complexes **4a–d**·H_2O intermediate values were obtained, in agreement with the expectation that the π-back-donation from rhodium to the carbene would be weaker in these complexes than in **3a–d**·H_2O because of the competitive back-donation to the π-acidic carbonyl ligands on the metal. An exception are complexes **3d**·H_2O and **4d**·H_2O, which featured nearly identical values for the $\nu(CO_{backbone})$ vibration. The reason for this behavior is not known. It is notable that in the quinone-annulated NHC system used by Bielawski for the evaluation of the metal-to-ligand π-back-bonding in similar rhodium complexes, the values of the $\nu(CO_{backbone})$ vibration spanned a range of 15 cm^{-1},[7a] whereas this range was even smaller for the ν(CN) vibrations of NHCs adorned with cyano functionalities on the backbone.[7c] Not surprisingly, the amido system reported herein proves much more sensitive to π-interactions, featuring $\nu(CO_{backbone})$ vibrations over a range of 75–95 cm^{-1}.

Table 4. Compilation of $\nu(CO_{backbone})$ values for **1a–d**, **3a–d**·H_2O, and **4a–d**·H_2O [cm^{-1}][a]

	a	b	c	d
1	1668.6	1679.6	1683.4	1681.3
3	1579.5	1596.6	1589.7	1605.4
4	1600.7	1614.4	1606.5	1603.7

[a] KBr pellets.

Whereas the large differences observed for the ν(CO) vibrations corresponding to the amido functionalities in compounds **1**, **3**, and **4** leave little doubt about the comparative π-donor ability of the metal centers (or the proton) in these complexes, the assessment of the influence of the N-substituents on the π-acceptor ability of the NHC ligand is hampered by the opposite trends that are expected: Under the influence of the increasingly electron-withdrawing effect of the N-substituents with increasing degree of fluorination, the π-donation from nitrogen to the CO group within the amido moiety is expected to decrease, resulting in an increase in the frequency of the ν(CO) vibration from derivatives **a** to **b** to **c** to **d**. This trend is confirmed relatively well by the values obtained for **1a–d** (Table 4). For derivatives **3** and **4**, however, the increasingly electron-withdrawing effect of the N-substituents with increasing degree of fluorination is also expected to increase the π-acidity of the ligand and hence the metal-to-ligand π-back-donation, resulting in an increase in the frequency of the ν(CO) vibration from derivatives **d** to **c** to **b** to **a**. Consequently, no consistent trend relating the π-accepting ability of the NHC-F_n^- ($n = 0$, 4, 6, and 10) ligands to the degree of fluorination of the N-substituents was observed in the IR spectra of these species.

NMR spectroscopy can also be used to assess the electron density on the metal center.[7c,32] An electron-rich metal center donates electron density into the antibonding orbital of the olefin in [Rh(cod)(L)(NHC)] complexes, resulting in a structure with more pronounced metallacyclopropane character, and hence a more significant upfield shift of the resonances corresponding to the olefin ligand from the alkene, towards the alkyl range. The ^1H and ^{13}C chemical shift values presented in Table 5 correspond to the *cis* and *trans* olefin moieties in **3a–d**. The systematic trend to lower-field chemical shifts displayed by all signals when going from **3a** to **3b**, **3c**, **3d** indicates a clear decrease in the electron density on the metal in this order. This trend is expect-

Table 5. Compilation of selected ^{1}H and ^{13}C spectroscopic chemical shift values for **3a–d**·H_2O and **4a–d**·H_2O [ppm][a]

	a	b	c	d
3, *trans*-CH_{COD}	4.01	4.16	4.27	4.47
3, *cis*-CH_{COD}	66.5	66.9	67.1	69.8
3, *trans*-CH_{COD}	92.2	95.5	96.1	99.7
3, N_2C	206.2	211.8	212.7	215.2
4, N_2C	199.1	200.0	200.7	203.4

[a] Recorded in [D_6]DMSO, except for **3d**, **4a**, and **4d**, which were recorded in [D_8]THF.

ed as a consequence of the decreased σ-donation and increased π-acceptance of the NHC ligands with increasing degree of fluorination. The trend is even more pronounced for the olefin group *trans* to the carbene ligand. NMR spectroscopy further confirms the efficiency of the fluoroaryl groups in tuning the electronic properties of the NHC ligand but does not provide a means for separating the σ and π components that produce this effect.

For a better understanding of the electronic effects that govern the bonding of the NHC ligands described herein to metals, a computational analysis of the model systems **N**

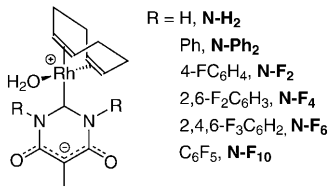

R = H, **N-H$_2$**
Ph, **N-Ph$_2$**
4-FC_6H_4, **N-F$_2$**
2,6-$F_2C_6H_3$, **N-F$_4$**
2,4,6-$F_3C_6H_2$, **N-F$_6$**
C_6F_5, **N-F$_{10}$**

was conducted. The calculated frontier orbitals for each carbene fragment were typical of other NHCs. The carbene frontier orbitals generally considered to play the most important role in the binding of these ligands to metals are π_{NC}, consisting of an in-phase stabilizing interaction between the occupied nitrogen p orbitals and the unoccupied carbene p orbital, σ_C, consisting of the occupied carbene σ-orbital, and a π^*_{NC}, consisting of an unoccupied π-orbital situated on the carbene carbon atom (Figure 5).

The HOMO of the NHC ligand in **N** is comprised of an in-phase interaction between the three sp^2 backbone carbon atoms, occupied by the resonating π-electrons in the anionic backbone fragment (Figure 5). The standard NHC σ_C, occupied by the carbene lone pair, comprises the HOMO-1. This ordering of the HOMOs of model system **N** is in agreement with the experimental evidence showing that the counterion in $[\mathbf{K_{Me}}]_3[Li(thf)_2]_3$ is coordinated to the oxygen centers adorning the backbone, and not the nucleophilic carbene center. The presence of this occupied MO higher in energy than the σ_C carbene orbital also suggests a reactive site in these carbenes, potentially available for further functionalization with electrophiles. The π_{NC} is also present and positioned well below the HOMO, which indicates a strongly stabilizing interaction. Finally, the unoccupied π^*_{CN} orbital situated on the carbene carbon atom is positioned at higher

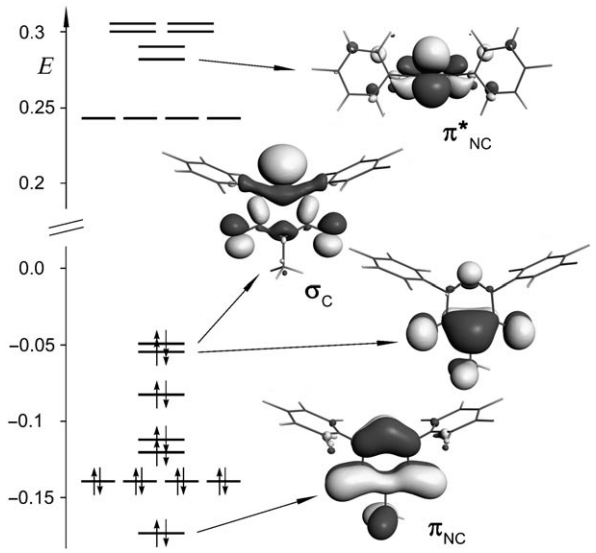

Figure 5. MO diagram depicting the energy levels and shape of the key frontier orbitals of the NHC ligands in systems **N**, exemplified for **N-F$_6$**. Energy in hartrees.

energy than the LUMO, which is composed of a quadruply degenerate set of MOs situated primarily on the phenyl rings. The relative energy levels of the frontier molecular orbitals σ_C and π^*_{CN} (Table 6) provide an indication regarding

Table 6. Energies of the σ_C MO, π^*_{CN} MO, and the σ_C–π^*_{CN} gap in the optimized structure of the free NHCs of compounds **N** [eV] and calculated Rh–C_{NHC} bond lengths (Å).

	$E(\sigma_C)$	$E(\pi^*_{CN})$	$E(\sigma_C)-E(\pi^*_{CN})$	Rh–C_{NHC}
N-H$_2$	−0.761	8.506	9.267	2.029
N-Ph$_2$	−0.999	8.155	9.154	2.072
N-F$_4$	−1.202	7.930	9.132	2.054
N-F$_2$	−1.371	7.899	9.270	2.070
N-F$_6$	−1.476	7.652	9.128	2.053
N-F$_{10}$	−1.947	7.320	9.267	2.064

the electron-donating or -accepting properties of the NHC. The general trend for the NHC ligands in the model compounds **N** is a decrease in the energy of σ_C and π^*_{CN} for increasingly electron-withdrawing N-substituents, reflecting diminished σ-donor and increased π-acceptor ability for ligands with higher degrees of fluorination. An exception is the difluorinated ligand in **N-F$_2$**, (Ar = 4-FC_6H_4) for which both orbitals lie slightly lower in energy than their counterparts in **N-F$_4$**, (Ar = 2,6-$F_2C_6H_3$), which suggests that the influence of the *para* substituents is particularly effective in altering the electronic properties of these ligands.

The NHC–metal bond was analyzed by using the extended transition-state natural orbitals for chemical valence (ETS-NOCV) scheme,[33] which provides a combined qualitative and quantitative picture of bonding. By using NOCVs, chemical bonds can be visualized by using the deformation density $\Delta\rho$, which is the difference in electron

density between the complex and the fragments that comprise the complex. On the criteria of associated eigenvalues and overall energy contribution, four NOCV pairs were identified as significant contributors to the NHC–Rh bond, in agreement with previous NOCV analyses of bonding in NHC–metal complexes.[6h] The four NOCV pairs consist of a σ-donation component and three back-bonding components, including two with π-symmetry, and one σ-component (Figure 6). The deformation density plot of the first NOCV pair ($\Delta\rho_{\sigma d}$) depicts σ-donation from the σ_C of the carbene fragment to the $d_x2_{-y}2$ orbital of the metal fragment. The second NOCV pair ($\Delta\rho_{\pi bd}$) shows the primary back-bonding component of the metal–NHC bond. The deformation density plot shows that electron density is transferred from the occupied d_{xy} orbital on the metal fragment to the empty carbene π^*_{CN} orbital. These two NOCV pairs, σ-donation, and π-back-donation represent the largest single contributors to the orbital interaction energy of the NHC–metal bond. The third and fourth NOCV pairs ($\Delta\rho_{\sigma bd}$ and $\Delta\rho_{\pi bd2}$) comprise smaller contributions to the NHC–metal bond and are considered as back-bonding components due to the outflow of density from the metal fragment and subsequent inflow to the carbene fragment. The sigma donor component ($\Delta\rho_{\sigma d}$) of the orbital interaction energy decreased with increased fluorination of the N-substituents, as expected given the σ-electron-withdrawing nature of fluorine (Table 7). Concomitantly, the electron-withdrawing substituents also result in a lower energy HOMO of the carbene fragment and, therefore, less favorable σ-donation.

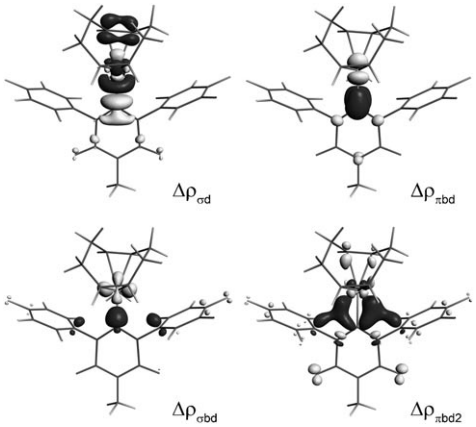

Figure 6. Deformation density plots of **N-F$_6$** describing the bond between the NHC and the metal fragment, including σ-donation ($\Delta\rho_{\sigma d}$), π-back-donation ($\Delta\rho_{\pi bd}$, $\Delta\rho_{\pi bd2}$), and σ-back-donation ($\Delta\rho_{\sigma bd}$). Dark grey indicates an increase in electron density (inflow, $\Delta\rho > 0$), whereas light grey represents a decrease (outflow, $\Delta\rho < 0$).

The primary π-back-donation component of the NHC–Rh bond ($\Delta E_{\pi bd}$) similarly responded to changes in the electron-donating and -withdrawing character of the N-substituents. Compounds **N-H$_2$**, **N-Ph$_2$**, and **N-F$_2$**, featured the smallest π-back-bonding contribution to the orbital interaction energy. The π-back-bonding contribution increased by as much as 1.5 kcal mol^{-1} in the more fluorinated analogues (Table 7). A small jump in π-back-bonding energy was observed when going from the *para*-fluorophenyl (**N-F$_2$**) to the 2,6-difluorophenyl N-substituents (**N-F$_4$**), but the energy remained relatively constant with further increases in the degree of fluorination, which suggests that for this particular set of compounds, 2,6-difluorophenyl N-substituents are sufficient to achieve the desired increase in π-accepting capabilities. This agreed well with the experimental observations, which failed to identify a consistent trend in the π-accepting abilities of carbenes NHC-F$_n^-$ ($n = 4$, 6, and 10), as monitored by the shift in the $\nu(CO_{backbone})$ vibration in compounds **1**, **3**, and **4** (Table 4) The two NOCV pairs comprising minor contributions to the NHC–Rh π-bond, $\Delta\rho_{\sigma bd}$ and $\Delta\rho_{\pi bd2}$ (Figure 6), do not follow a discernable trend with increasing electron-withdrawing or -donating strength of the N-substituents, which suggests that these contributions are independent of small changes in the electronic environment of the NHC. Therefore, it seems that the classic π-back-bonding contribution to the NHC–metal bond, wherein electron density is transferred from the metal fragment to the π^*_{CN} MO of the carbene, represents the only tunable back-bonding component.

Table 7. ETS-NOCV energy decomposition[a] of the metal–NHC bond in complexes **N**. All energy contributions are in kcal mol^{-1}.

	ΔE_{Pauli}	ΔE_{steric}[b]	ΔE_{orb}[c]	$\Delta E_{\sigma d}$	$\Delta E_{\pi bd}$	$\Delta E_{\sigma bd}$	$\Delta E_{\pi bd2}$	ΔE_{rest}	ΔE_{prep}	ΔE_{int}[d]
N-H$_2$	201.1	−56.1	−83.6	−53.2	−10.6	−4.9	−3.0	−11.8	7.7	−139.7
N-Ph$_2$	187.2	−44.7	−92.2	−47.9	−10.1	−6.1	−3.8	−23.5	9.2	−137.0
N-F$_4$	194.2	−47.8	−92.5	−46.2	−11.4	−5.4	−3.2	−25.4	7.2	−140.3
N-F$_2$	186.8	−41.7	−91.1	−47.6	−10.1	−5.7	−3.8	−22.8	11.9	−132.7
N-F$_6$	192.8	−44.6	−91.4	−45.9	−11.6	−5.4	−3.2	−24.5	7.5	−136.1
N-F$_{10}$	177.7	−41.7	−84.0	−45.3	−11.0	−5.3	−3.2	−18.0	5.8	−125.7

[a] The electrostatic interaction energy (ΔE_{elstat}), the Pauli repulsion contribution (ΔE_{Pauli}), the preparation energy (ΔE_{prep}), and the orbital interaction energy (ΔE_{int}) are all defined elsewhere.[40] [b] $\Delta E_{steric} = \Delta E_{Pauli} + \Delta E_{elstat}$; it is usually destabilizing as is ΔE_{prep} above representing the energy required to distort the two fragments to the structures they have in the final complex. [c] $\Delta E_{orb} = \Delta E_{\sigma} + \Delta E_{\pi bd} + \Delta E_{\sigma bd} + \Delta E_{\pi bd2} + \Delta E_{rest}$. All orbital interaction contributions are stabilizing and explained in text. [d] $\Delta E_{int} = \Delta E_{steric} + \Delta E_{orb} + \Delta E_{prep}$.

It is noteworthy that in all compounds **N** featuring substituted or unsubstituted phenyl N groups, the ΔE_{rest}, which constitutes the rest of the orbital interaction energy, represents a considerable portion of the total orbital interaction energy. The large ΔE_{rest} contribution to the total orbital interaction energy is due to both weak interactions between the NHC and other auxiliary ligands on the metal fragment, as well as relief of Pauli repulsion. For example, compounds **N-F$_n$**, $n = 4$, 6, 10, which all contain fluorine in the *ortho* position on the phenyl N-substituent, feature a hydrogen-bond-

ing interaction between the water ligand and the *ortho*-fluorine, as proposed above based on geometry and metric parameters (Figure 7). This interaction represents a transfer of electron density to the space between the *ortho*-fluorine and

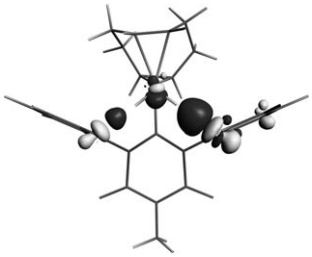

Figure 7. Deformation density plot of compound **N-F$_6$**, depicting hydrogen bonding between hydrogen on the water ligand and the *ortho*-fluorine of the N-substituent.

the hydrogen of the water ligand, indicative of a weak hydrogen-bonding interaction. The largest contributor to the ΔE_{rest} is, however, a rearrangement of electron density within both the NHC and metal fragment to relieve the Pauli repulsion between occupied orbitals. The vast majority of remaining NOCV pairs consist of density changes on the phenyl rings of the NHC and the metal fragment to alleviate repulsion between the two fragments. To isolate this effect, compound **N-H$_2$**, which features hydrogen rather than aryl N-substituents, was used for comparison. In all cases, the ΔE_{rest} was considerably smaller (by as much as 13.6 kcal mol^{-1}) for the complex lacking aryl substituents, supporting the conclusion that a large portion of the orbital interaction energy is comprised of relief of Pauli repulsion.

Conclusion

In the first systematic study of the effect that fluorination of the N-substituents has on the electronic properties of NHCs, a series of anionic ligands from this class with six-membered ligand frameworks and varying degrees of fluorination, including the first *N,N′*-bis(perfluorophenyl) representative, have been incorporated in rhodium complexes. The structural and spectroscopic studies of these complexes revealed that fluorination has a considerable influence on the electronic properties of the metal center and can be used to efficiently tune this property over a broad range. The influence of the degree of fluorination beyond the 2,6-difluorophenyl derivatives to the 2,4,6-trifluoro and pentafluoro analogues was less extensive but it nevertheless followed the expected trend. In addition, the highly electronegative *ortho*-fluorine atoms on the N-aryl substituents were found to directly alter the properties of the coordination pocket of the NHC ligand, rendering the rhodium complexes highly hydrophilic by forming hydrogen bonds with the water ligand coordinated to the metal. All fluoroaryl groups provided substantial steric protection to the carbene center, the steric demand of the investigated ligands, NHC-F$_n^-$ ($n=4$, 6, and 10), being comparable to that of 1,3-bis(2,6-diisopropylphenyl)imidazolidin-2-ylidene (IPr).

The computational analysis of model systems **N** confirmed that both the σ-donation and π-back-donation components, which could not be separated experimentally, can be electronically tuned by altering the N-substituents. The effect was demonstrated by energy changes in both the frontier orbitals of the carbene ligand, and through changes in individual bonding contributions established by the ETS-NOCV analyses. Electron-withdrawing N-substituents decreased the energy of the both the σ_C and π^*_{CN} molecular orbitals. Through the ETS-NOCV analysis, it was determined that with increasingly more electron-withdrawing substituents, the σ-donation orbital interaction energy decreases, whereas the π-back-donation energy increases. Thus, the electron-withdrawing or electron-donating nature of the N-substituents was found to be useful in manipulating the energies of the individual bonding contributions.

Experimental Section

General: Unless otherwise noted, all operations were performed under an argon atmosphere by using standard Schlenk and glove box techniques. Solvents were dried and deoxygenated prior to use, with the exception of [D$_5$]DMSO, which contained residual water. Fluorinated formamidines were prepared by using a slight modification of the procedure reported for the preparation of *N,N′*-bis(pentafluorophenyl)formamidine,[18] which was very effective for the synthesis of formamidines with a higher degree of fluorination but not for their nonfluorinated analogues. In a typical trial, one drop of concentrated hydrochloric acid was added to a neat stoichiometric mixture of the aniline and triethylorthoformate. Upon stirring for several minutes, the mixture solidified, yielding the desired formamidines in near quantitative yields after washing with hexanes. *tert*-Butylmalonyl chloride was prepared according to the published procedures.[34] All other reagents were purchased from commercial suppliers. NMR spectra were collected on a Bruker Advance RDQ-400 spectrometer and calibrated with respect to [D$_7$]THF (^{1}H, $\delta=3.58$ ppm), [D$_8$]THF (^{13}C, $\delta=67.57$ ppm), $CDHCl_2$ (^{1}H, $\delta=5.32$ ppm), CD_2Cl_2 (^{13}C, $\delta=54.00$ ppm), [D$_5$]DMSO (^{1}H, $\delta=2.50$ ppm), and [D$_6$]DMSO (^{13}C, $\delta=39.51$ ppm). ^{19}F NMR spectra were calibrated with respect to C_6F_6 (^{19}F, $\delta=-164.9$ ppm). Mass spectra and elemental analyses were performed by the Analytical Instrumentation Laboratory, Department of Chemistry, University of Calgary (Canada).

(NHC-F$_0$)H (1a): *N,N′*-Bis(2,6-dimethylphenyl)formamidine (408 mg, 1.62 mmol) was added to a solution of *tert*-butylmalonyl chloride (256 mg, 1.30 mmol) in THF (25 mL). The mixture was stirred for 1 h, after which time, triethylamine (0.36 mL, 2.60 mmol) was added to the solution, resulting in the formation of a precipitate of triethylamine•hydrochloride. The precipitate was filtered off and the volatiles were removed from the filtrate under high vacuum, allowing for the isolation of the title product as a yellow/brown solid (476 mg, 97%). ^{1}H NMR (400 MHz, CD_2Cl_2): $\delta=1.41$ (s, 9H; *tBu*), 2.16 (s, 12H; $C_6H_3Me_2$), 7.19–7.17 (m, 4H; *m*-$C_6H_3Me_2$), 7.32–7.28 (m, 2H; *p*-$C_6H_3Me_2$), 8.09 ppm (s, 1H; N_2CH); ^{13}C{H} NMR (101 MHz, CD_2Cl_2): $\delta=18.1$ (s; *p*-$C_6H_3(CH_3)_2$), 30.3 (s; $C(CH_3)_3$), 35.0 (s; $C(CH_3)_3$), 104.8 (s; *C*-*t*Bu), 129.1 (s; C_6H_3), 130.3 (s; C_6H_3), 136.0 (s; C_6H_3), 136.3 (s; C_6H_3), 148.0 (s; *C*O), 157.9 ppm (s; N_2CH); IR (KBr pellet): $\tilde{\nu}=1668.6$ cm^{-1} (vs; CO); MS (EI): *m/z*: 376 $[M]^+$.

(NHC-F$_4$)H (1b): *N,N′*-Bis(2,6-difluorophenyl)formamidine (532 mg, 1.98 mmol) was added to a solution of *tert*-butylmalonyl chloride (521 mg, 2.64 mmol) in THF (25 mL). The mixture was stirred for 1 h, after which time, triethylamine (0.55 mL, 3.96 mmol) was added to the

solution, resulting in the formation of a precipitate of triethylamine·hydrochloride. The precipitate was filtered off and the volatiles were removed from the filtrate under high vacuum, allowing for the isolation of the title product as a yellow solid (420 mg, 54%). ^{1}H NMR (400 MHz, [D$_8$]THF): δ=1.41 (s, 9H; *tBu*), 7.22–7.18 (m, 4H; *m*-$C_6F_2H_3$), 7.59–7.54 (m, 2H; *p*-$C_6F_2H_3$), 9.38 ppm (s, 1H; N_2CH); ^{19}F NMR (376 MHz, [D$_8$]THF): δ=−120.09 ppm (t, $^3J_{FH}$=7.5 Hz; *o*-$C_6F_2H_3$); ^{13}C{^{1}H} NMR (101 MHz, [D$_8$]THF): δ=30.7 (s; $C(CH_3)_3$), 35.4 (s; $C(CH_3)_3$), 101.4 (s; *C*-*t*Bu), 113.0 (dd, $^2J_{CF}$=20.3, $^4J_{CF}$=3.0 Hz; *m*-$C_6F_2H_3$), 115.4 (t, $^2J_{CF}$=16.8 Hz; *i*-$C_6F_2H_3$), 133.1 (t, $^3J_{CF}$=10.1 Hz; *p*-$C_6F_2H_3$), 153.5 (s; *C*O), 156.6 (s; N_2CH), 159.6 ppm (dd, $^1J_{CF}$=253.2 Hz; *o*-$C_6F_2H_3$); IR (KBr pellet): $\tilde{\nu}$=1679.6 cm^{-1} (vs; CO); elemental analysis calcd (%) for $C_{20}H_{16}N_2O_2F_4$: C 61.22, H 4.11, N 7.14; found: C 60.87, H 4.21, N 6.97; MS (EI): *m*/*z*: 392.35 [*M*]$^+$.

(NHC-F$_6$)H (1c): *N,N*′-Bis(2,4,6-difluorophenyl)formamidine (889 mg, 2.92 mmol) was added to a solution of *tert*-butylmalonyl chloride (768 mg, 3.90 mmol) in THF (25 mL). The mixture was stirred for 1 h, after which time, triethylamine (0.81 mL, 5.84 mmol) was added to the solution, resulting in the formation of a precipitate of triethylamine·hydrochloride. The precipitate was filtered off and the volatiles were removed from the filtrate under high vacuum, yielding a solid. Recrystallization of the crude solid from THF allowed for the isolation of the title product as yellow block crystals (1.013 g, 81%). ^{1}H NMR (400 MHz, [D$_8$]THF): δ=1.39 (s, 9H; *tBu*), 7.24–7.20 (m, 4H; *m*-$C_6F_3H_2$), 9.36 ppm (s, 1H; N_2CH); ^{19}F NMR (376 MHz, [D$_8$]THF): δ=−116.44 (t, 2F, $^4J_{FF}$=7.5 Hz; *o*-$C_6F_3H_2$), −104.59 ppm (tt, 1F, $^3J_{FH}$=8.8, $^4J_{FF}$=7.1 Hz; *p*-$C_6F_3H_2$); ^{13}C{^{1}H} NMR (101 MHz, CD_2Cl_2): δ=30.3 (s; $C(CH_3)_3$), 35.0 (s; $C(CH_3)_3$), 102.0 (s; *C*-*t*Bu), 102.0 (td, $^2J_{CF}$=25.8, $^4J_{CF}$=4.0 Hz; *m*-$C_6F_3H_2$), 110.9 (td, $^2J_{CF}$=16.6, $^4J_{CF}$=5.2 Hz; *i*-$C_6F_3H_2$), 151.1 (s; *C*O), 156.2 (s; N_2CH), 159.2 (dm, $^1J_{CF}$=256.5, $^3J_{CF}$=5.6 Hz; *o*-$C_6F_3H_2$), 164.1 ppm (dt, $^1J_{CF}$=256.5, $^3J_{CF}$=14.6 Hz; *p*-$C_6F_3H_2$); IR (KBr pellet): $\tilde{\nu}$=1683.4 cm^{-1} (vs; CO); elemental analysis calcd (%) for $C_{20}H_{16}N_2O_2F_4$: C 56.08, H 3.29, N 6.54; found: C 56.50, H 3.72, N 6.14; MS (EI): *m*/*z*: 428.33 [*M*]$^+$.

(NHC-F$_{10}$)H (1d): *N,N*′-Bis(pentafluorophenyl)formamidine (832 mg, 2.21 mmol) was added to a solution of *tert*-butylmalonyl chloride (583 mg, 2.96 mmol) in THF (20 mL). The mixture was stirred for 1 h, after which time, triethylamine was added to the solution, resulting in the formation of a precipitate of triethylamine·hydrochloride. The precipitate was filtered off and the volatiles were removed from the filtrate under high vacuum, allowing for the isolation of the title product as a yellow solid (980 mg, 89%). ^{1}H NMR (400 MHz, [D$_8$]THF): δ=1.39 (s, 9H; *tBu*); 9.61 ppm (s, 1H; N_2CH); ^{19}F NMR (376 MHz, CD_2Cl_2): δ=−160.34 (tm, 4F, $^2J_{FF}$=20.7 Hz; *m*-C_6F_5), −149.08 (t, 2F, $^2J_{FF}$=20.7 Hz; *p*-C_6F_5), −144.34 ppm (dm, 4F, $^2J_{FF}$=18.8 Hz; *o*-C_6F_5); ^{13}C{^{1}H} NMR (101 MHz, CD_2Cl_2): δ=30.0 (s; $C(CH_3)_3$), 35.2 (s; $C(CH_3)_3$), 102.7 (s; *C*-*t*Bu), 111.6 (tm, $^2J_{CF}$=15.2 Hz; *i*-C_6F_5), 138.6 (dm, $^1J_{CF}$=260.6 Hz; *m*-C_6F_5), 143.6 (dtm, $^1J_{CF}$=260.6, $^2J_{CF}$=13.1 Hz; *p*-C_6F_5), 144.4 (dm, $^1J_{CF}$=255.5 Hz; *o*-C_6F_5), 151.6 (s; *C*O), 155.4 ppm (s; N_2CH); IR (KBr pellet): $\tilde{\nu}$=1681.3 cm^{-1} (vs; CO); elemental analysis calcd (%) for $C_{20}H_{16}N_2O_2F_4$: C 48.01, H 2.01, N 5.60; found: C 48.02, H 2.06, N 5.08; MS (EI): *m*/*z*: 502.39 [*M*]$^+$.

(NHC-F$_4$)K (2b): KHMDS (13 mg, 0.065 mmol) was added to a THF solution (0.5 mL) of (NHC-F$_4$)H (**1b**) (25 mg, 0.064 mmol) and the mixture was agitated. Removal of the volatiles in vacuo resulted in the isolation of the title product as a white powder in quantitative yield. Major species: ^{1}H NMR (400 MHz, [D$_8$]THF): δ=1.37 (s, 9H; *tBu*), 6.93–6.89 (m, 4H; *m*-$C_6F_2H_3$), 7.21 ppm (m, 2H; *p*-$C_6F_2H_3$); ^{19}F NMR (376 MHz, [D$_8$]THF): δ=−120.40 ppm (t, 4F, $^3J_{HF}$=6.4 Hz; *m*-$C_6F_2H_3$); ^{13}C{H} NMR (101 MHz, [D$_8$]THF): δ=31.9 (s; $C(CH_3)_3$), 34.6 (s; *C*-$(CH_3)_3$), 98.9 (s; *C*-*t*Bu), 111.9 (dd, $^2J_{CF}$=17.9, $^4J_{CF}$=6.3 Hz; *m*-$C_6F_2H_3$), 125.6 (t, $^2J_{CF}$=16.1 Hz; *i*-$C_6F_2H_3$), 128.0 (t, $^3J_{CF}$=9.6 Hz; *p*-$C_6F_2H_3$), 160.7 (dd, $^1J_{CF}$=249.1, $^3J_{CF}$=5.1 Hz; *o*-$C_6F_2H_3$), 161.5 (s; *C*O), 244.5 ppm (s, N_2C); minor species: ^{1}H NMR (400 MHz, [D$_8$]THF): δ=1.33 (9H, s; *tBu*), 6.93–6.89 (4H, m; *m*-$C_6F_2H_3$), 7.21 ppm (2H, m; *p*-$C_6F_2H_3$); ^{19}F NMR (376 MHz, [D$_8$]THF): δ=−116.61, −111.50 ppm (4F; *m*-$C_6F_2H_3$); ^{13}C{H} NMR (101 MHz, [D$_8$]THF): δ=32.8 (s; $C(CH_3)_3$), 34.4 (s; $C(CH_3)_3$), 84.4, 85.7 (s; *C*-*t*Bu), 165.3 ppm (s, *C*O).

[Rh(cod)(NHC-F$_0$)] (3a·H$_2$O): KHMDS (13 mg, 0.066 mmol) was added to a THF solution (0.5 mL) of (NHC-F$_0$)H (**1a**) (25 mg, 0.066 mmol) and the mixture was agitated. Solid [{RhCl(cod)}$_2$] (16 mg, 0.033 mmol) was added to the reaction mixture immediately. Upon mixing, the title product deposited out of solution as an orange crystalline solid. The supernatant solvent was decanted off and the crystals were dried under high vacuum (24 mg, 60%). ESI-MS analysis suggests that this solid is free of coordinated water; however, upon dissolving the sample in [D$_6$]DMSO for NMR spectroscopic analysis, one equivalent of water can be seen in the ^{1}H NMR spectrum of the complex. ^{1}H NMR (400 MHz, [D$_6$]DMSO): δ=1.28 (s, 9H; *tBu*), 1.44–1.35 (m, 8H; CH_{2COD}), 1.98 (brs, 6H; $C_6H_3Me_2$), 2.37 (brs, 6H; $C_6H_3Me_2$), 3.09 (brs, 2H; CH_{COD}), 3.29 (s, 2H; H_2O), 4.01 (brs, 2H; CH_{COD}), 7.07–7.08 (m, 4H; *m*-$C_6H_3Me_2$), 7.16–7.19 ppm (m, 2H; *p*-$C_6H_3Me_2$); ^{13}C{H} NMR (101 MHz, [D$_6$]DMSO): δ=18.9 (brs; *p*-$C_6H_3(CH_3)_2$), 20.3 (brs; *p*-$C_6H_3(CH_3)_2$), 26.9 (s; CH_{2COD}), 30.7 (s; $C(CH_3)_3$), 33.2 (s; $C(CH_3)_3$), 66.5 (d, $^1J_{CRh}$=15.0 Hz; CH_{COD}), 92.2 (d, $^1J_{CRh}$=7.3 Hz; CH_{COD}), 96.1 (s; *C*-*t*Bu), 126.4 (brs; C_6H_3), 126.4 (s; C_6H_3), 127.7 (brs; C_6H_3), 135.9 (brs; C_6H_3), 138.5 (brs; C_6H_3), 142.3 (s; C_6H_3), 160.1 (s; *C*O), 206.2 ppm (d, $^1J_{CRh}$=47.9 Hz; N_2C-Rh); IR (KBr pellet): $\tilde{\nu}$=1579.5 cm^{-1} (vs; CO); MS (ESI): *m*/*z*: 587.7 [*M*−H$_2$O+H]$^+$.

[Rh(cod)(NHC-F$_4$)(OH$_2$)] (3b·H$_2$O): KHMDS (16 mg, 0.080 mmol) was added to a THF solution (0.5 mL) of (NHC-F$_4$)H (**1b**) (30 mg, 0.076 mmol) and the mixture was agitated. Solid [{RhCl(cod)}$_2$] (19 mg, 0.039 mmol) was immediately added to the reaction mixture. Upon mixing, **3b** deposited immediately as an orange solid. The supernatant solvent was decanted and the crystals were dried under high vacuum. ^{1}H NMR (400 MHz, [D$_6$]DMSO): δ=1.24 (s, 9H; *tBu*), 1.59–1.39 (m, 8H; CH_{2COD}), 3.27 (brs, 2H; CH_{COD}), 3.31 (s, 2H; H_2O), 4.16 (brs, 2H; CH_{COD}), 7.13 (dd, 2H, $^3J_{HF}$=8.5, $^3J_{HH}$=8.5 Hz; *m*-$C_6F_2H_3$), 7.21 (dd, 2H, $^3J_{HF}$=9.0, $^3J_{HH}$=9.0 Hz; *m*-$C_6F_2H_3$), 7.51 ppm (tt, 2H, $^3J_{HH}$=8.3, $^4J_{HF}$=6.2 Hz; *p*-$C_6F_2H_3$); ^{19}F NMR (376 MHz, [D$_6$]DMSO): δ=−115.52 (m, 2F; *o*-$C_6F_2H_3$), −107.26 ppm (m, 2F; *o*-$C_6F_2H_3$); ^{13}C{^{1}H} NMR (101 MHz, [D$_6$]DMSO): δ=27.1 (s; CH_{2COD}), 30.7 (s; $C(CH_3)_3$), 31.9 (s; CH_{2COD}), 33.1 (s; $C(CH_3)_3$), 66.9 (dd, $^1J_{CRh}$=11.5, J_{CF}=9.0 Hz; CH_{COD}), 94.6 (s; *C*-*t*Bu), 95.5 (d, $^1J_{CRh}$=7.1 Hz; CH_{COD}), 110.5 (dd, $^2J_{CF}$=19.2, $^4J_{CF}$=2.0 Hz; *m*-$C_6F_2H_3$), 112.1 (dd, $^2J_{CF}$=8.1, $^4J_{CF}$=2.0 Hz; *m*-$C_6F_2H_3$), 120.3 (t, $^2J_{CF}$=16.7 Hz; *i*-$C_6F_2H_3$), 129.2 (t, $^3J_{CF}$=9.6 Hz; *p*-$C_6F_2H_3$), 158.0 (dd, $^1J_{CF}$=27.3, $^3J_{CF}$=5.1 Hz; *o*-$C_6F_2H_3$), 159.2 (s; *C*O), 160.52 (dd, $^1J_{CF}$=35.4, $^3J_{CF}$=5.1 Hz; *o*-$C_6F_2H_3$), 211.8 ppm (d, $^1J_{CRh}$=48.5 Hz; N_2C-Rh); IR (KBr pellet): $\tilde{\nu}$=1596.6 cm^{-1} (vs; CO); elemental analysis calcd (%) for $C_{28}H_{29}N_2O_3F_4Rh·C_4H_8O$: C 55.50, H 5.39, N 4.04; found: C 56.45, H 5.23, N 4.57; MS (EI): *m*/*z*: 601.86 [*M*−H$_2$O]$^+$.

[Rh(cod)(NHC-F$_6$)(OH$_2$)] (3c·H$_2$O): KHMDS (14 mg, 0.070 mmol) was added to a THF solution (0.5 mL) of (NHC-F$_6$)H (**1c**) (30 mg, 0.070 mmol) and the mixture was agitated. Solid [{RhCl(cod)}$_2$] (17 mg, 0.035 mmol) was added to the reaction mixture immediately. Upon mixing, the title product deposited out of solution as an orange solid. The supernatant solvent was decanted and the crystals were dried under high vacuum. X-ray quality crystals were obtained by slow evaporation of the solvent from a solution of **3c** in THF. ^{1}H NMR (400 MHz, [D$_6$]DMSO): δ=1.24 (s, 9H; *tBu*), 1.84–1.40 (m, 8H; CH_{2COD}), 3.24 (brs, 2H; CH_{COD}), 3.28 (s, 2H; H_2O), 4.27 (brs, 2H; CH_{COD}), 7.21 (ddm, 2H, $^3J_{HF}$=9.1, $^3J_{HF}$=9.1 Hz; *m*-$C_6F_3H_2$), 7.32 ppm (ddm, 2H, $^3J_{HF}$=9.5, $^3J_{HF}$=9.5 Hz; *m*-$C_6F_3H_2$); ^{19}F NMR (376 MHz, [D$_6$]DMSO): δ=−112.41 (m, 2F; *o*-$C_6F_3H_2$), −109.56 (m, 2F; *p*-$C_6F_3H_2$), −103.51 ppm (m, 2F; *o*-$C_6F_3H_2$); ^{13}C{^{1}H} NMR (101 MHz, [D$_6$]DMSO): δ=27.2 (s; CH_{2COD}), 30.6 (s; C-$(CH_3)_3$), 32.0 (s; CH_{2COD}), 33.1 (s; $C(CH_3)_3$), 67.1 (dd; $^1J_{CRh}$=13.9, J_{CF}=8.5 Hz; CH_{COD}), 94.5 (s; *C*-*t*Bu), 96.1 (d, $^1J_{CRh}$=6.1 Hz; CH_{COD}), 99.4 (td, $^2J_{CF}$=26.4, $^4J_{CF}$=2.8 Hz; *m*-$C_6F_3H_2$), 100.7 (td, $^2J_{CF}$=25.6, $^4J_{CF}$=2.6 Hz; *m*-$C_6F_3H_2$), 117.41 (td, $^2J_{CF}$=17.2, $^4J_{CF}$=5.1 Hz; *i*-$C_6F_3H_2$), 159.0 (s; *C*O), 159.2 (ddd, $^1J_{CF}$=247.6, $^3J_{CF}$=16.2, $^3J_{CF}$=8.3 Hz; *o*-$C_6F_3H_2$), 159.7 (ddd, $^1J_{CF}$=256.5, $^3J_{CF}$=15.9, $^3J_{CF}$=7.3 Hz; *o*-$C_6F_3H_2$), 161.3 (dt, $^1J_{CF}$=247.5, $^3J_{CF}$=15.2 Hz; *p*-$C_6F_3H_2$), 212.7 ppm (d, $^1J_{CRh}$=49.4 Hz; N_2C-Rh); IR (KBr pellet): $\tilde{\nu}$=1589.7 cm^{-1} (vs; CO); MS (EI): *m*/*z*: 637.89 [*M*−H$_2$O]$^+$.

[Rh(cod)(NHC-F$_{10}$)] (3d) and [Rh(cod)(NHC-F$_{10}$)(OH$_2$)] (3d·H$_2$O): KHMDS (10 mg, 0.050 mmol) was added to a THF solution (0.5 mL) of (NHC-F$_{10}$)H (**1d**) (25 mg, 0.050 mmol) and the mixture was agitated.

Solid [{RhCl(cod)}$_2$] (12 mg, 0.025 mmol) was added to the reaction mixture immediately. The mixture was allowed to react for 90 min at room temperature and the volatiles were subsequently removed under high vacuum affording [Rh(cod)(NHC-F$_{10}$)] as an orange solid in quantitative yield. ^{1}H NMR (400 MHz, [D$_8$]THF): δ = 1.30 (s, 9H; *tBu*), 1.77 (m, 8H; CH_{2COD}), 3.34 (br s, 2H; CH_{COD}), 4.47 ppm (br s, 2H; CH_{COD}); ^{19}F NMR (376 MHz, [D$_8$]THF): δ = −168.13 (ddm, 2F, $^3J_{FF}$ = 22.4, $^3J_{FF}$ = 22.2 Hz; *m*-C$_6F_5$), −166.18 (ddm, 2F, $^3J_{FF}$ = 23.5, $^3J_{FF}$ = 22.3 Hz; *m*-C$_6F_5$), −159.11 (t, 2F, $^3J_{FF}$ = 21.3 Hz; *p*-C$_6F_5$), −142.61 (dm, 2F, $^3J_{FF}$ = 23.5 Hz; *o*-C$_6F_5$), −135.24 ppm (dm, 2F, $^3J_{FF}$ = 24.5 Hz; *o*-C$_6F_5$); ^{13}C{^{1}H} NMR (101 MHz, [D$_8$]THF): δ = 28.8 (s; CH_{2COD}), 31.2 (s; C(CH_3)$_3$), 33.6 (s; *C*(CH$_3$)$_3$), 34.5 (s; CH_{2COD}), 69.8 (dd, $^1J_{CRh}$ = 11.8, J_{CF} = 9.3 Hz; CH_{COD}), 96.2 (s; *C*-*t*Bu), 99.7 (d, $^1J_{CRh}$ = 7.0 Hz; CH_{COD}), 120.5 (tm, $^2J_{CF}$ = 15.2, $^3J_{CF}$ = 4.0 Hz; *i*-C$_6$F$_5$), 138.3 (dddm, $^1J_{CF}$ = 246.5, $^2J_{CF}$ = 14.5, $^3J_{CF}$ = 4.8 Hz; *m*-C$_6$F$_5$), 139.1 (dddm, $^1J_{CF}$ = 247.6, $^2J_{CF}$ = 13.0, $^3J_{CF}$ = 3.6 Hz; *m*-C$_6$F$_5$), 141.9 (dtm, $^1J_{CF}$ = 251.5, $^3J_{CF}$ = 13.1 Hz; *p*-C$_6$F$_5$), 146.1 (dm, $^1J_{CF}$ = 240.4 Hz; *o*-C$_6$F$_5$), 146.5 (dm, $^1J_{CF}$ = 253.5 Hz; *o*-C$_6$F$_5$), 160.0 (s; *C*O), 215.2 ppm (d, $^1J_{CRh}$ = 48.3 Hz; N$_2$C-Rh); IR (KBr pellet): $\tilde{\nu}$ = 1605.4 cm^{-1} (vs; CO); MS (EI): *m*/*z*: 709.90 [*M*−H$_2$O]$^+$; X-ray quality crystals were grown by slow evaporation of the solvent through a rubber septum outside the glovebox, resulting in coordination of adventitious water to the rhodium center to give [Rh(cod)(NHC-F$_{10}$)(OH$_2$)].

[Rh(CO)$_2$(NHC-F$_0$)] (4a) and [Rh(CO)$_2$(NHC-F$_0$)(OH$_2$)] (4a·H$_2$O): KHMDS (13 mg, 0.066 mmol) was added to a solution of (NHC-F$_0$)H (**1a**) (25 mg, 0.066 mmol) in THF (0.5 mL) and the mixture was agitated. Solid [{RhCl(CO)$_2$}$_2$] (13 mg, 0.033 mmol) was immediately added and the mixture was allowed to react for 90 min at room temperature. Removal of the volatiles under high vacuum left behind a mixture of [Rh(CO)$_2$(NHC-F$_0$)] and potassium chloride as an orange solid in quantitative yield. The crude solid was washed with cold diethyl ether and dried under high vacuum. ^{1}H NMR (400 MHz, [D$_8$]THF): δ = 1.45 (s, 9H; *tBu*), 2.27 (s, 6H; C$_6$H$_3$*Me*$_2$), 2.35 (s, 6H; C$_6$H$_3$*Me*$_2$), 7.06–7.08 (m, 2H; *m*-C$_6$*H*$_3$Me$_2$), 7.12–7.13 (m, 2H; *p*-C$_6$*H*$_3$Me$_2$), 7.22–7.18 ppm (m, 2H; *p*-C$_6$*H*$_3$Me$_2$); ^{13}C{H} NMR (101 MHz, [D$_8$]THF): δ = 20.4 (s; *p*-C$_6$H$_3$-(*C*H$_3$)$_2$), 19.0 (s; *p*-C$_6$H$_3$(*C*H$_3$)$_2$), 31.4 (s; C(*C*H$_3$)$_3$), 34.9 (s; *C*(CH$_3$)$_3$), 100.6 (s; *C*-*t*Bu), 128.3 (s; *C*$_6$H$_3$), 128.6 (s; *C*$_6$H$_3$), 129.0 (s; *C*$_6$H$_3$), 136.4 (s; *C*$_6$H$_3$), 139.3 (s; *C*$_6$H$_3$), 142.9 (s; *C*$_6$H$_3$), 161.9 (s; *C*O), 185.2 (d, $^1J_{CRh}$ = 75.7 Hz; Rh*C*O), 187.8 (d, $^1J_{CRh}$ = 53.3 Hz; Rh*C*O), 199.1 ppm (d, $^1J_{CRh}$ = 41.8 Hz; N$_2$*C*-Rh); IR (KBr pellet): $\tilde{\nu}$ = 1600.7 (vs; CO$_{backbone}$), 1994.9 cm^{-1} (vs; RhCO), 2074.4 cm^{-1} (vs; RhCO); MS (EI): *m*/*z*: 569.1 [*M*+Cl]$^-$.

[Rh(CO)$_2$(NHC-F$_4$)] (4b) and [Rh(CO)$_2$(NHC-F$_4$)(OH$_2$)] (4b·H$_2$O): Carbon monoxide was bubbled through a [D$_6$]DMSO solution of [Rh(cod)(NHC-F$_4$)(OH$_2$)] (**3b**) (15 mg, 24 mmol) for 2 h, after which time, the ^{1}H, ^{19}F, and ^{13}C NMR spectra were obtained. The NMR spectra demonstrated the quantitative conversion of the starting material to the title product. The complex could be isolated as a solid by trapping the free carbene in situ as follows: KHMDS (16 mg, 0.080 mmol) was added to a THF solution (0.5 mL) of (NHC-F$_4$)H (**1b**) (15 mg, 0.038 mmol) and the mixture was agitated. Solid [{RhCl(CO)$_2$}$_2$] (7.5 mg, 0.019 mmol) was immediately added to the reaction mixture, which was then allowed to react for 90 min at room temperature. The volatiles were subsequently removed under high vacuum affording a mixture of [Rh(CO)$_2$(NHC-F$_4$)] and potassium chloride as an orange solid in quantitative yield. The crude solid was washed with cold diethyl ether and dried under high vacuum. ^{1}H NMR (400 MHz, [D$_6$]DMSO): δ = 1.29 (s, 9H; *tBu*), 3.33 (s, 2H; H$_2$O), 7.13 (dd, 2H, $^3J_{HF}$ = 8.5, $^3J_{HF}$ = 8.5 Hz; *m*-C$_6$F$_2$*H*$_3$), 7.21 (dd, 2H, $^3J_{HF}$ = 8.7, $^3J_{HF}$ = 8.7 Hz; *m*-C$_6$F$_2$*H*$_3$), 7.54–7.47 ppm (m, 2H; *p*-C$_6$F$_2$*H*$_3$); ^{19}F NMR (376 MHz, [D$_6$]DMSO): δ = −118.14 (s, 2F; *o*-C$_6$F$_2$H$_3$), −112.26 ppm (s, 2F; *o*-C$_6$F$_2$H$_3$); ^{13}C{^{1}H} NMR (101 MHz, [D$_6$]DMSO): δ = 30.7 (s; C(CH$_3$)$_3$), 33.4 (s; *C*(CH$_3$)$_3$), 96.5 (s; *C*-*t*Bu), 111.2 (dd, $^2J_{CF}$ = 64.5, $^4J_{CF}$ = 2.9 Hz; *m*-C$_6$F$_2$H$_3$), 111.8 (dd, $^2J_{CF}$ = 63.7, $^4J_{CF}$ = 2.9 Hz; *m*-C$_6$F$_2$H$_3$), 119.3 (t, $^2J_{CF}$ = 16.1 Hz; *i*-C$_6$F$_2$H$_3$), 130.2 (t, $^3J_{CF}$ = 10.0 Hz; *p*-C$_6$F$_2$H$_3$), 158.1 (dd, $^1J_{CF}$ = 247.0, $^3J_{CF}$ = 5.0 Hz; *o*-C$_6$F$_2$H$_3$), 158.6 (s; *C*O), 158.8 (dd, $^1J_{CF}$ = 253.0, $^3J_{CF}$ = 4.0 Hz; *o*-C$_6$F$_2$H$_3$), 182.2 (br d, $^1J_{CRh}$ = 76.5 Hz; RhCO), 186.8 (d, $^1J_{CRh}$ = 53.3 Hz; RhCO), 200.0 ppm (d, $^1J_{CRh}$ = 42.0 Hz; N$_2$*C*-Rh); IR (KBr pellet): $\tilde{\nu}$ = 1614.4 (vs; C$_2$CO), 2013.1 (vs; RhCO), 2083.3 cm^{-1} (vs; RhCO); MS (EI): *m*/*z*: 550.08 [*M*−H$_2$O]$^+$.

[Rh(CO)$_2$(NHC-F$_6$)] (4c) and [Rh(CO)$_2$(NHC-F$_6$)(OH$_2$)] (4c·H$_2$O): In an NMR tube, carbon monoxide was passed through a solution of [Rh(cod)(NHC-F$_6$)(OH$_2$)] (**3c**) (15 mg, 23 mmol) in [D$_6$]DMSO (1 mL) for 2 h, after which time, the ^{1}H, ^{19}F, and ^{13}C NMR spectra were recorded and demonstrated the quantitative conversion of the starting material to the title product. The complex could be isolated as a solid by trapping the free carbene in situ as follows: KHMDS (7.0 mg, 0.035 mmol) was added to a THF solution (0.5 mL) of (NHC-F$_6$)H (**1c**) (15 mg, 0.035 mmol) and the mixture was agitated. Solid [{RhCl(CO)$_2$}$_2$] (6.8 mg, 0.018 mmol) was immediately added and the mixture was allowed to react for 90 min at room temperature. Removal of the volatiles under high vacuum left behind a mixture of **4c** and potassium chloride as an orange solid in quantitative yield, which was washed with cold diethyl ether and dried under high vacuum. ^{1}H NMR (400 MHz, [D$_6$]DMSO): δ = 1.29 (s, 9H; *tBu*), 3.34 (s, 2H; H$_2$O), 7.28 (dd, 2H, $^3J_{HF}$ = 9.0, $^3J_{HF}$ = 9.0 Hz; *m*-C$_6$F$_3$*H*$_2$), 7.36 ppm (dd, 2H, $^3J_{HF}$ = 9.2, $^3J_{HF}$ = 9.2 Hz; *m*-C$_6$F$_3$*H*$_2$); ^{19}F NMR (376 MHz, [D$_6$]DMSO): δ = −114.94 (s, 2F; *p*-C$_6$F$_3$H$_2$), −108.69 (s, 2F; *o*-C$_6$F$_3$H$_2$), −107.30 ppm (s, 2F; *o*-C$_6$F$_3$H$_2$); ^{13}C{^{1}H} NMR (101 MHz, [D$_6$]DMSO): δ = 30.5 (s; C(*C*H$_3$)$_3$), 33.4 (s; *C*-(CH$_3$)$_3$), 96.5 (s; *C*-*t*Bu), 101.2–100.1 (m; *m*-C$_6$F$_3$H$_2$), 116.3 (td, $^2J_{CF}$ = 16.6, $^4J_{CF}$ = 5.0 Hz; *i*-C$_6$F$_3$H$_2$), 158.2 (ddd, $^1J_{CF}$ = 248.0, $^3J_{CF}$ = 16.1, $^3J_{CF}$ = 7.0 Hz; *o*-C$_6$F$_3$H$_2$), 158.4 (s; *C*O), 159.1 (ddd, $^1J_{CF}$ = 253.5, $^3J_{CF}$ = 16.1, $^3J_{CF}$ = 7.0 Hz; *o*-C$_6$F$_3$H$_2$), 161.6 (dt, $^1J_{CF}$ = 247.5, $^3J_{CF}$ = 15.1 Hz; *p*-C$_6$F$_3$H$_2$), 182.0 (dt, $^1J_{CRh}$ = 75.5, J_{CF} = 3.9 Hz; Rh*C*O), 186.6 (d, $^1J_{CRh}$ = 54.3 Hz; RhCO), 200.7 ppm (d, $^1J_{CRh}$ = 40.8 Hz; N$_2$*C*-Rh); IR (KBr pellet): $\tilde{\nu}$ = 1606.5 (vs; C$_2$CO), 2015.2 (vs; RhCO), 2085.0 cm^{-1} (vs; RhCO); MS (ESI-): *m*/*z*: 621.02 [*M*+Cl]$^-$.

[Rh(CO)$_2$(NHC-F$_{10}$)] (4d) [Rh(CO)$_2$(NHC-F$_{10}$)(OH$_2$)] (4d·H$_2$O): KHMDS (8.0 mg, 0.040 mmol) was added to a solution of (NHC-F$_{10}$)H (**1d**) (20 mg, 0.040 mmol) in THF (0.5 mL) and the mixture was agitated. Solid [{RhCl(CO)$_2$}$_2$] (7.8 mg, 0.020 mmol) was immediately added and the mixture was allowed to react for 90 min at room temperature. Removal of the volatiles under high vacuum left behind a mixture of [Rh(CO)$_2$(NHC-F$_{10}$)] and potassium chloride as an orange solid in quantitative yield. The crude solid was washed with cold diethyl ether and dried under high vacuum. ^{1}H NMR (400 MHz, [D$_8$]THF): δ = 1.35 ppm (s, 9H; *tBu*); ^{19}F NMR (376 MHz, [D$_8$]THF): δ = −166.46 (ddd, 2F, $^3J_{FF}$ = 22.2, $^3J_{FF}$ = 22.2, $^4J_{FF}$ = 3.0 Hz; *m*-C$_6F_5$), −165.90 (ddd, 2F, $^3J_{FF}$ = 22.4, $^3J_{FF}$ = 22.4, $^4J_{FF}$ = 2.9 Hz; *m*-C$_6F_5$), −157.33 (t, 2F, $^3J_{FF}$ = 21.3 Hz; *p*-C$_6F_5$), −144.96 (dm, 2F, $^2J_{FF}$ = 23.0 Hz; *o*-C$_6F_5$), −138.40 ppm (dt, 2F, $^2J_{FF}$ = 22.6, $^4J_{FF}$ = 3.8 Hz; *o*-C$_6F_5$); ^{13}C{^{1}H} NMR (101 MHz, [D$_8$]THF): δ = 31.12 (s; C(*C*H$_3$)$_3$), 34.8 (s; *C*(CH$_3$)$_3$), 98.0 (s; *C*-*t*Bu), 119.5 (tm, $^2J_{CF}$ = 12.6 Hz; *i*-C$_6$F$_5$), 138.5 (dm, $^1J_{CF}$ = 250.5 Hz; *m*-C$_6$F$_5$), 138.9 (dm, $^1J_{CF}$ = 245.5 Hz; *m*-C$_6$F$_5$), 142.5 (ddd, $^1J_{CF}$ = 252.5, $^3J_{CF}$ = 13.6 Hz; *p*-C$_6$F$_5$), 145.2 (dm, $^1J_{CF}$ = 258.5 Hz; *o*-C$_6$F$_5$), 146.1 (dm, $^1J_{CF}$ = 254.5 Hz; *o*-C$_6$F$_5$), 159.5 (s; *C*O), 183.1 (dt, $^1J_{CRh}$ = 73.4, J_{CF} = 4.4 Hz; Rh-*C*O), 187.5 (d, $^1J_{CRh}$ = 53.3 Hz; Rh-*C*O), 203.4 ppm (d, $^1J_{CRh}$ = 40.6 Hz; N$_2$*C*-Rh); IR (KBr pellet): $\tilde{\nu}$ = 1603.7 (vs; C$_2$CO), 2015.4 (vs; RhCO), 2091.2 cm^{-1} (vs; RhCO); MS (ESI-): *m*/*z*: 692.94 [*M*+Cl]$^-$.

X-ray crystallographic studies of 1c, 3b, 3c, and 3d: Non-hydrogen atoms were refined anisotropically. Hydrogen atoms were included at geometrically calculated positions and refined by using the riding model. CCDC-781511, 781512, 781513, and 781514 contain the supplementary crystallographic data for compounds **1c**, **3b**, **3c**, and **3d**, respectively. These data can be obtained free of charge from The Cambridge Crystallographic Data Centre via www.ccdc.cam.ac.uk/data_request/cif.

*Compound **1c***: C$_{20}$H$_{14}$F$_6$N$_2$O$_2$; 173 K; 0.40×0.40×0.10 mm; monoclinic; space group $P2_1/c$; a = 14.7240(4), b = 10.3760(4), c = 19.5350(6) Å; α = γ = 90, β = 129.098(2)°; V = 2316.16(13) Å^3; Z = 4; ρ_{calcd} = 1.228 g cm^{-3}; 1.79 ≤ θ ≤ 27.38°; R_1 = 0.0683 (I > 2σ(I)), wR_2 = 0.1779 (all data); residual electron density = 0.278/−0.294 e Å^{-3}.

*Compound **3b***: C$_{28}$H$_{29}$F$_4$N$_2$O$_3$Rh; 173 K; 0.10×0.08×0.04 mm; monoclinic; space group $P2_1/c$; a = 10.5780(3), b = 21.0850(9), c = 15.8840(6) Å; α = γ = 90, β = 98.911(2)°; V = 3500.0(2) Å^3; Z = 4; ρ_{calcd} = 1.177 g cm^{-3}; 1.93 ≤ θ ≤ 27.48°; R_1 = 0.0643 (I > 2σ(I)), wR_2 = 0.1785 (all data); residual electron density = 1.892/−0.750 e Å^{-3}; Mo$_{K\alpha}$ radiation (λ = 0.71073 Å).

*Compound **3c***: C$_{28}$H$_{27}$F$_6$N$_2$O$_3$Rh; 173 K; 0.16×0.04×0.02 mm; monoclinic; space group $P2_1/c$; a = 10.2740(4), b = 14.2740(7), c = 21.5330(10) Å;

$\alpha=\gamma=90$, $\beta=92.457(3)°$; $V=3154.9(2)$ Å^3; $Z=4$; $\rho_{calcd}=1.382$ g cm^{-3}; $1.71\leq\theta\leq27.53°$; $R_1=0.0730$ ($I>2\sigma(I)$), $wR_2=0.1757$ (all data); residual electron density = 0.668/−0.597 e Å^{-3}.

Compound ***3d***: $C_{56}H_{46}F_{20}N_4O_6Rh_2$; 173 K; 0.80×0.60×0.20 mm; triclinic; space group $P-1$; $a=13.4550(4)$, $b=15.9910(4)$, $c=18.0140(4)$ Å; $\alpha=107.963(2)$, $\beta=96.243(2)$, $\gamma=112.6360(10)°$; $V=3286.77(15)$ Å^3; $Z=2$; $\rho_{calcd}=1.472$ g cm^{-3}; $1.23\leq\theta\leq27.55°$; $R_1=0.0688$ ($I>2\sigma(I)$), $wR_2=0.1928$ (all data); residual electron density = 1.162/−0.831 e Å^{-3}.

Computational details: All density functional theory calculations were carried out by using the Amsterdam Density Functional (ADF) program[35] and the Becke–Perdew exchange correlation functional[36] was applied. A standard Slater-type triple-ζ basis set with one set of polarization functions was used for all atoms. Scalar relativistic effects were included in all systems studied by using the ZORA approximation.[37] The NHC–metal bond of the optimized structures was analyzed by using the ETS-NOCV scheme, as previously described.[40]

Acknowledgements

This work was supported by the Natural Sciences and Engineering Research Council of Canada, the Canada Foundation for Innovation, and the Alberta Science and Research Investments Program. C.J.K. thanks the NSERC for two USRA scholarships and J.B.G. thanks CONACYT for a PhD scholarship.

[1] C. Präsang, B. Donnadieu, G. Bertrand, *J. Am. Chem. Soc.* **2005**, *127*, 10182–10183.

[2] a) D. Bourissou, O. Guerret, F. P. Gabbaï, G. Bertrand, *Chem. Rev.* **2000**, *100*, 39–92; b) *Carbene Chemistry: From Fleeting Intermediates to Powerful Reagents* (Ed.: G. Bertrand), Marcel Dekker, New York, **2002**; c) Y. Canac, M. Soleilhavoup, S. Conejero, G. Bertrand, *J. Organomet. Chem.* **2004**, *689*, 3857–3865; d) F. E. Hahn, M. C. Jahnke, *Angew. Chem.* **2008**, *120*, 3166–3216; *Angew. Chem. Int. Ed.* **2008**, *47*, 3122–3172; e) K. Hirai, T. Itoh, H. Tomioka, *Chem. Rev.* **2009**, *109*, 3275–3332; f) J. Vignolle, X. Cattoën, D. Bourissou, *Chem. Rev.* **2009**, *109*, 3333–3384.

[3] a) W. A. Herrmann, C. Köcher, *Angew. Chem.* **1997**, *109*, 2256–2282; *Angew. Chem. Int. Ed. Engl.* **1997**, *36*, 2162–2187; b) A. J. Arduengo III, *Acc. Chem. Res.* **1999**, *32*, 913–921; c) W. A. Herrmann, *Angew. Chem.* **2002**, *114*, 1342–1363; *Angew. Chem. Int. Ed.* **2002**, *41*, 1290–1309; d) R. W. Alder, M. E. Blake, L. Chaker, J. N. Harvey, F. Paolini, J. Schütz, *Angew. Chem.* **2004**, *116*, 6020–6036; *Angew. Chem. Int. Ed.* **2004**, *43*, 5896–5911; e) V. Nair, S. Bindu, V. Sreekumar, *Angew. Chem.* **2004**, *116*, 5240–5245; *Angew. Chem. Int. Ed.* **2004**, *43*, 5130–5135; f) D. Enders, O. Niemeier, A. Henseler, *Chem. Rev.* **2007**, *107*, 5606–5655; g) O. Kühl, *Chem. Soc. Rev.* **2007**, *36*, 592–607; h) D. Tapu, D. A. Dixon, C. Roe, *Chem. Rev.* **2009**, *109*, 3385–3407; i) O. Schuster, L. Yang, H. G. Raubenheimer, M. Albrecht, *Chem. Rev.* **2009**, *109*, 3445–3478.

[4] a) L. Jafarpour, S. P. Nolan, *J. Organomet. Chem.* **2001**, *617–618*, 17–27; b) D. Enders, H. Gielen, *J. Organomet. Chem.* **2001**, *617–618*, 70–80; c) A. C. Hillier, G. A. Grasa, M. S. Viciu, H. M. Lee, C. Yang, S. P. Nolan, *J. Organomet. Chem.* **2002**, *653*, 69–82; d) E. Peris, R. H. Crabtree, *Coord. Chem. Rev.* **2004**, *248*, 2239–2246; e) C. M. Crudden, D. P. Allen, *Coord. Chem. Rev.* **2004**, *248*, 2247–2273; f) V. César, S. Bellemin-Laponnaz, L. H. Gade, *Chem. Soc. Rev.* **2004**, *33*, 619–636; g) N. M. Scott, S. P. Nolan, *Eur. J. Inorg. Chem.* **2005**, 1815–1828; h) *N-Heterocyclic Carbenes in Synthesis* (Ed.: S. P. Nolan), Wiley-VCH, Weinheim, **2006**; i) *Top. Organomet. Chem Vol. 21: N-Heterocyclic Carbenes in Transition Metal Catalysis* (Ed.: F. Glorius), Springer, New York, **2007**; j) E. A. B. Kantchev, C. J. O'Brien, M. G. Organ, *Angew. Chem.* **2007**, *119*, 2824–2870; *Angew. Chem. Int. Ed.* **2007**, *46*, 2768–2813; k) N. Marion, S. P. Nolan, *Acc. Chem. Res.* **2008**, *41*, 1440–1449; l) S. Würtz, F. Glorius, *Acc. Chem. Res.* **2008**, *41*, 1523–1533; m) J. M. Praetorius, C. M. Crudden, *Dalton Trans.* **2008**, 4079–4094; n) J. C. Y. Lin, R. T. W. Huang, C. S. Lee, A. Bhattacharyya, W. S. Hwang, I. J. B. Lin, *Chem. Rev.* **2009**, *109*, 3561–3598.

[5] a) A. R. Chianese, X. Li, M. C. Janzen, J. W. Faller, R. H. Crabtree, *Organometallics* **2003**, *22*, 1663–1667; b) W. A. Herrmann, J. Schütz, G. D. Frey, E. Herdtweck, *Organometallics* **2006**, *25*, 2437–2448; c) A. Fürstner, M. Alcarazo, H. Krause, C. W. Lehmann, *J. Am. Chem. Soc.* **2007**, *129*, 12676–12677; d) M. Iglesias, D. J. Beetstra, A. Stasch, P. N. Horton, M. B. Hursthouse, S. J. Coles, K. J. Cavell, A. Dervisi, I. A. Fallis, *Organometallics* **2007**, *26*, 4800–4909; e) R. A. Kelly III, H. Clavier, S. Giudice, N. M. Scott, E. D. Stevens, J. Bordner, I. Samardjiev, C. D. Hoff, L. Cavallo, S. P. Nolan, *Organometallics* **2008**, *27*, 202–210; f) S. Wolf, H. Plenio, *J. Organomet. Chem.* **2009**, *694*, 1487–1492; g) D. G. Gusev, *Organometallics* **2009**, *28*, 6458–6461.

[6] a) X. Hu, I. Castro-Rodriguez, K. Olsen, K. Meyer, *Organometallics* **2004**, *23*, 755–764; b) D. Nemcsok, K. Wichmann, G. Frenking, *Organometallics* **2004**, *23*, 3640–3646; c) S. K. Schneider, P. Roembke, G. R. Julius, C. Loschen, H. G. Raubenheimer, G. Frenking, W. A. Herrmann, *Eur. J. Inorg. Chem.* **2005**, 2973–2977; d) H. Jacobsen, A. Correa, C. Costabile, L. Cavallo, *J. Organomet. Chem.* **2006**, *691*, 4350–4358; e) R. Tonner, G. Heydenrych, G. Frenking, *Chem. Asian J.* **2007**, *2*, 1555–1567; f) A. Kausamo, H. M. Tuononen, K. E. Krahulic, R. Roesler, *Inorg. Chem.* **2008**, *47*, 1145–1154; g) U. Radius, M. Bickelhaupt, *Organometallics* **2008**, *27*, 3410–3414; h) M. Srebro, A. Michalak, *Inorg. Chem.* **2009**, *48*, 5361–5369; i) N. S. Antonova, J. J. Carbó, J. M. Poblet, *Organometallics* **2009**, *28*, 4283–4287.

[7] a) M. D. Sanderson, J. W. Camplain, C. W. Bielawski, *J. Am. Chem. Soc.* **2006**, *128*, 16514–16515; b) L. Mercs, G. Labat, A. Neels, A. Ehlers, M. Albrecht, *Organometallics* **2006**, *25*, 5648–5656; c) D. M. Khramov, V. M. Lynch, C. W. Bielawski, *Organometallics* **2007**, *26*, 6042–6049; d) A. Bittermann, P. Härter, E. Herdtweck, S. D. Hoffmann, W. A. Herrmann, *J. Organomet. Chem.* **2008**, *693*, 2079–2090.

[8] a) S. Díez-González, S. P. Nolan, *Coord. Chem. Rev.* **2007**, *251*, 874–883; b) H. Jacobsen, A. Correa, A. Poater, C. Costabile, L. Cavallo, *Coord. Chem. Rev.* **2009**, *253*, 687–703.

[9] C. A. Tolman, *J. Am. Chem. Soc.* **1970**, *92*, 2953–2956.

[10] a) K. Randell, M. J. Stanford, G. J. Clarkson, J. P. Rourke, *J. Organomet. Chem.* **2006**, *691*, 3411–3415; b) S. C. Zinner, C. F. Rentzsch, E. Herdtweck, W. A. Herrmann, F. E. Kühn, *Dalton Trans.* **2009**, 7055–7062.

[11] a) J. W. Ogle, J. Zhang, J. H. Reibenspies, K. A. Abboud, S. A. Miller, *Org. Lett.* **2008**, *10*, 3677–3680; b) J. W. Ogle, S. A. Miller, *Chem. Commun.* **2009**, 5728–5730.

[12] J. Ruiz, B. F. Perandones, G. García, M. E. G. Mosquera, *Organometallics* **2007**, *26*, 5687–5695.

[13] a) T. Ritter, M. W. Day, R. H. Grubbs, *J. Am. Chem. Soc.* **2006**, *128*, 11768–11769; b) J. M. Berlin, K. Campbell, T. Ritter, T. W. Funk, A. Chlenov, R. H. Grubbs, *Org. Lett.* **2007**, *9*, 1339–1342; c) D. R. Anderson, D. J. O'Leary, R. H. Grubbs, *Chem. Eur. J.* **2008**, *14*, 7536–7544.

[14] S. Leuthäußer, V. Schmidts, C. M. Thiele, H. Plenio, *Chem. Eur. J.* **2008**, *14*, 5465–5481.

[15] G. C. Vougioukalakis, R. H. Grubbs, *Organometallics* **2007**, *26*, 2469–2472.

[16] G. C. Vougioukalakis, R. H. Grubbs, *Chem. Eur. J.* **2008**, *14*, 7545–7556.

[17] a) L. Xu, W. Chen, J. F. Bickley, A. Steiner, J. Xiao, *J. Organomet. Chem.* **2000**, *598*, 409–416; b) S. Burling, M. F. Mahon, S. P. Reade, M. K. Whittlesey, *Organometallics* **2006**, *25*, 3761–3767.

[18] H. E. Abdou, A. A. Mohamed, J. M. López-de-Luzuriaga, J. P. Fackler, Jr., *J. Cluster Sci.* **2004**, *15*, 397–411.

[19] M. G. Hobbs, T. D. Forster, J. Borau-Garcia, C. J. Knapp, H. M. Tuononen, R. Roesler, *New J. Chem.* **2010**, *34*, 1295–1308.

[20] V. César, N. Lugan, G. Lavigne, *J. Am. Chem. Soc.* **2008**, *130*, 11286–11287.

[21] a) T. W. Hudnall, C. W. Bielawski, *J. Am. Chem. Soc.* **2009**, *131*, 16039–16041; b) V. César, N. Lugan, G. Lavigne, *Eur. J. Inorg.*

Chem. **2010**, 361–365; c) T. W. Hudnall, E. J. Moorhead, D. G. Gusev, C. W. Bielawski, *J. Org. Chem.* **2010**, *75*, 2763–2766; d) T. W. Hudnall, J. P. Moerdyk, C. W. Bielawski, *Chem. Commun.* **2010**, *46*, 4288–4290.

[22] a) L. Benhamou, V. César, H. Gornitzka, N. Lugan, G. Lavigne, *Chem. Commun.* **2009**, 4720–4722; b) A. T. Biju, K. Hirano, R. Fröhlich, F. Glorius, *Chem. Asian J.* **2009**, *4*, 1786–1789; c) L. Benhamou, N. Vujkovic, V. César, H. Gornitzka, N. Lugan, G. Lavigne, *Organometallics* **2010**, *29*, 2616–2630.

[23] B. Bak, L. Hansen-Nygaard, J. Rastrup-Andersen, *J. Mol. Spectrosc.* **1958**, *2*, 361–368.

[24] Data was obtained from the Cambridge Structural Database by using ConQuest and Vista, see a) D. A. Fletcher, R. F. McMeeking, D. Parkin, *J. Chem. Inf. Model.* **1996**, *36*, 746–749; b) F. H. Allen, *Acta Crystallogr. B* **2002**, *58*, 380–388; c) I. J. Bruno, J. C. Cole, P. R. Edgington, M. Kessler, C. F. Macrae, P. McCabe, J. Pearson and R. Taylor, *Acta Crystallogr. B* **2002**, *58*, 389–397.

[25] K. Tamagawa, T. Iijima, M. Kimura, *J. Mol. Struct.* **1976**, *30*, 243–253.

[26] S. F. Lincoln, A. M. Hounslow, N. J. Maeji, T. W. Hambley, M. R. Snow, A. J. Jones, *Aust. J. Chem.* **1983**, *36*, 1865–1871.

[27] a) J. Chen, J. Reibenspies, A. Derecskei-Kovacs, K. Burgess, *Chem. Commun.* **1999**, 2501–2502; b) X. Xie, Y. Yuan, R. Krüger, M. Bröring, *Magn. Reson. Chem.* **2009**, *47*, 1024–1030.

[28] E. D'Oria, J. J. Novoa, *CrystEngComm* **2008**, *10*, 423–436.

[29] a) J. D. Dunitz, R. Taylor, *Chem. Eur. J.* **1997**, *3*, 89–98; b) H. Takemura, M. Kaneko, K. Sakob, T. Iwanagac, *New J. Chem.* **2009**, *33*, 2004–2006.

[30] a) M. K. Denk, A. Hezarkhani, F.-L. Zheng, *Eur. J. Inorg. Chem.* **2007**, 3527–3534; b) L. Cavallo, A. Correa, C. Costabile, H. Jacobsen, *J. Organomet. Chem.* **2005**, *690*, 5407–5413; c) S. Díez-González, S. P. Nolan, *Coord. Chem. Rev.* **2007**, *251*, 874–883; d) L. H. Gade, S. Bellemin-Laponnaz, *Top. Organomet. Chem.* **2007**, *21*, 117–157; e) A. Poater, F. Ragone, S. Giudice, C. Costabile, R. Dorta, S. P. Nolan, L. Cavallo, *Organometallics* **2008**, *27*, 2679–2681; f) O. Kühl, *Coord. Chem. Rev.* **2009**, *253*, 2481–2492.

[31] a) A. Poater, B. Cosenza, A. Correa, S. Giudice, F. Ragone, V. Scarano, L. Cavallo, *Eur. J. Inorg. Chem.* **2009**, 1759–1766; b) http://www.molnac.unisa.it/OMtools/sambvca.php; c) H. Clavier, S. P. Nolan, *Chem. Commun.* **2010**, *46*, 841–861.

[32] R. H. Crabtree, J. M. Quirk, *J. Organomet. Chem.* **1980**, *199*, 99–106.

[33] M. P. Mitoraj, A. Michalak, T. Ziegler, *J. Chem. Theory Comput.* **2009**, *5*, 962–975.

[34] C. Holmberg, *Liebigs Ann. Chem.* **1981**, 748–760.

[35] a) G. te Velde, F. M. Bickelhaupt, E. J. Baerends, C. Fonseca Guerra, S. J. A. Van Gisbergen, J. G. Snijders, T. Ziegler, *J. Comput. Chem.* **2001**, *22*, 931–967, and references therein; b) E. J. Baerends, D. E. Ellis, P. Ros, *Chem. Phys.* **1973**, *2*, 41–51; c) E. J. Baerends, P. Ros, *Chem. Phys.* **1973**, *2*, 52–59; d) G. te Velde, E. J. Baerends, *J. Comput. Phys.* **1992**, *99*, 84–98; e) C. G. Fonseca, O. Visser, J. G. Snijders, G. te Velde, E. J. Baerends in *Methods and Techniques in Computational Chemistry, METECC-95* (Eds.: E. Clementi, G. Corongiu), STEF, Cagliari, Italy, **1995,** p. 305.

[36] a) A. Becke, *Phys. Rev. A* **1988**, *38*, 3098–3100; b) J. P. Perdew, *Phys. Rev. B* **1986**, *34*, 7406–7406.

[37] a) E. van Lenthe, E. J. Baerends, J. G. Snijders, *J. Chem. Phys.* **1993**, *99*, 4597–4610; b) E. van Lenthe, E. J. Baerends, J. G. Snijders, *J. Chem. Phys.* **1994**, *101*, 9783–9792; c) E. van Lenthe, R. van Leeuwen, E. J. Baerends, J. G. Snijders, *Int. J. Quantum Chem.* **1996**, *57*, 281–293.

[38] A. J. Arduengo III, R. Krafczyk, R. Schmutzler, H. A. Craig, J. R. Goerlich, W. J. Marshall, M. Unverzagt, *Tetrahedron* **1999**, *55*, 14523–14534.

[39] A. J. Arduengo III, S. F. Gamper, M. Tamm, J. C. Calabrese, F. Davidson, H. A. Craig, *J. Am. Chem. Soc.* **1995**, *117*, 572–573.

[40] S. I. Lee, S. Y. Park, J. H. Park, I. G. Jung, S. Y. Choi, Y. K. Chung, B. Y. Lee, *J. Org. Chem.* **2006**, *71*, 91–95.

[41] P. A. Evans, E. W. Baum, A. N. Fazal, M. Pink, *Chem. Commun.* **2005**, 63–65.

[42] M. Alcarazo, R. Fernández, E. Álvarez, J. M. Lassaletta, *J. Organomet. Chem.* **2005**, *690*, 5979–5988.

[43] K. Denk, P. Sirsch, W. A. Herrmann, *J. Organomet. Chem.* **2002**, *649*, 219–224.

[44] M. Mayr, K. Wurst, K.-H. Ongania, M. R. Buchmeiser, *Chem. Eur. J.* **2004**, *10*, 1256–1266.

Received: June 15, 2010
Published online: October 27, 2010

